Supporting information

Benzosuberyl installed "Sandwich" type unsymmetrical α-diimine nickel precatalysts for synthesizing plastomeric to elastomeric polyethylene

Aibo Zhou,[a,b] Rongyan Yuan,[b] Qaiser Mahmood,[b,*] Shifang Yuan,[a,*] Yizhou Wang,[c] Zexu Hu,[b] Song Zou,[c] Tongling Liang,[c] Wen-Hua Sun [b,c,*]

[a] Institute of Applied Chemistry, The School of Chemistry and Chemical Engineering, Shanxi University, Taiyuan 030006, China.
[b] Chemistry and Chemical Engineering Guangdong Laboratory, Shantou, 515031, China.
[c] Key Laboratory of Engineering Plastics, Institute of Chemistry, Chinese Academy of Sciences, Beijing, 100190.
*Corresponding authors; Email address: qaiser@ccelab.com.cn (Q. Mahmood); yuansf@sxu.edu.cn (S. Yuan), whsun@iccas.ac.cn (W.-H. Sun)

Contents

1. General conditions

All experiments involving compounds with high sensitivity to air and/or moisture were carried out in a nitrogen-purged environment, employing standard Schlenk techniques to ensure the stability of chemical reactions and the accuracy of experimental results. Toluene for polymerization was dried using sodium and distilled under a nitrogen atmosphere. MAO (1.67 M in toluene), MMAO (1.93 M in heptane), DMAC (0.9 M in heptane), DEAC (2.0 M in hexane) and EASC (0.4 M in hexane) were purchased from Macklin Corp. High-purity ethylene was purchased from Guangdong Jieyang Petrochemical Company. Other chemical reagents were purchased from Acros, Macklin, and Aladdin suppliers. The ^{1}H and ^{13}C NMR spectra of organic compounds were measured at room temperature on a Bruker DMX 600 MHz spectrometer. The thermo scientific/flashsmart element analyzer was used for element analysis. Utilizing 1,2,4-trichlorobenzene as the eluent, the molecular weight (Mw) and polydispersity index (PDI) of the polymer were precisely measured via PL-GPC220 at a temperature of 150°C. The melting point of the polymer was determined using Differential Scanning Calorimetry (DSC). The aforementioned melting point data were derived from the second scan run on the PerkinElmer DSC-7. Typically, about 10 mg of polyethylene sample was heated to 160°C at a heating rate of 20°C min^{-1}, kept at 160°C for 5 minutes to remove its thermal history, and then cooled at a rate of 10°C min^{-1} to 25°C. High-temperature ^{13}C NMR of the polyethylene was recorded on the Bruker AVANCE III 500 MHz at 110 ℃ in o-dichlorobenzene-d4 with TMS as an internal standard. The ^{1}H NMR spectra of the polyethylene were recorded on a Bruker DMX 600 MHz instrument at 80 °C in deuterated tetrachloroethane with TMS as an internal standard. Chemical shift was expressed in ppm, and coupling constant was expressed in Hz.2,4,6-tris(5-dibenzosuberyl)aniline **(1)** was synthesized using the method described in the reported literature[1].

2. Typical procedure for ethylene polymerization

The polymerization process at 10 atm ethylene pressure was conducted in a 250 mL stainless steel autoclave equipped with an ethylene pressure control system, a mechanical stirrer, and a temperature controller. Initially, the autoclave was dried, then purged twice with nitrogen and once with ethylene under reduced pressure to ensure an inert environment. the complex (2.0 μmol) was dissolved in 30 mL of toluene and injected into the autoclave at the required reaction temperature. An additional 30 mL of toluene was added for washing purposes. Next, the appropriate amount of co-catalyst

(MAO, MMAO, DMAC, DEAC, EASC) and more toluene were added successively to reach a total volume of 100 mL. The autoclave was immediately pressurized with 10 atm of ethylene, and stirring was initiated. After the desired reaction time, the ethylene pressure was released, and the reaction was quenched by adding 10% hydrochloric acid in ethanol. The resulting polymer was collected, washed with ethanol, dried under reduced pressure at room temperature, and then weighed.

3. X-ray crystallographic studies

Single crystals of **Ni^{iPr}**, **Ni^{PhF}** and **Ni^{PhOMe}**, suitable for X-ray analysis, were successfully grown by carefully layering hexane onto their respective dichloromethane solutions, all conducted at room temperature. The single-crystal X-ray diffraction analysis of **Ni^{iPr}**, **Ni^{PhF}** and **Ni^{PhOMe}** complexes were conducted using a Rigaku Sealed Tube CCD (Saturn 724+) diffractometer, Japan. The diffractometer employed graphite-monochromated Cu-Kα radiation with a wavelength (λ) of 0.71073 Å. The measurements were performed at a temperature of 170 (±10) K. The determination of cell parameters was a critical part of the process, achieved through global refinement based on the positions of reflections from a single scan of all collected reflections. We meticulously accounted for various effects in our analysis, including Lorentz and polarization, and applied empirical absorption corrections to the intensity data. The structures of **Ni^{iPr}**, **Ni^{PhF}** and **Ni^{PhOMe}** were identified via direct methods and further refined via full-matrix least squares fitting on F2. In our structural model, hydrogen atoms were positioned based on theoretical calculations, while all non-hydrogen atoms were refined anisotropically to achieve a precise understanding of their spatial arrangement. The structural solution and refinement for each complex were carried out using SHELXT (Sheldrick) software. The solvent molecules, which do not influence the geometry of the main compound, were also processed using SHELXT [2]. The crystal data and processing parameters for **Ni^{iPr}**, **Ni^{PhF}** and **Ni^{PhOMe}** are presented in Table S1.

4. Crystal data and structural refinements for complexes

Table S1. Crystal data and structural refinements for **Ni^{iPr}, Ni^{PhF}** and **Ni^{PhOMe}**

	Ni^{iPr}	**Ni^{PhF}**	**Ni^{PhOMe}**
CCDC	2372213	2372214	2372215
Bond precision	C-C = 0.0105	C-C = 0.0148	C-C = 0.0088
Empirical formula	$C_{66}H_{54}Br_2N_2Ni$	$C_{69}H_{51}Br_2FN_2Ni$	$C_{70}H_{54}Br_2N_2NiO$

Formula weight	1093.61	1145.65	1157.68
Temperature/K	169.99(10)	170.00(10)	170.00(10)
Crystal system	monoclinic	monoclinic	monoclinic
Space group	P_c	$P2_1/c$	I_a
a/Å	17.2648(2)	18.9938(8)	20.7377(2)
b/Å	21.1889(2)	15.5349(4)	12.96667(17)
c/Å	14.87016(16)	21.2740(6)	22.3479(3)
α/°	90	90	90
β/°	92.1506(11)	100.450(3)	99.2173(11)
γ/°	90	90	90
Volume/Å^3	5436.00(12)	6173.1(3)	5931.75(13)
Z	2	4	4
ρ_{calc}g/cm^3	1.336	1.233	1.296
μ/mm^{-1}	2.551	2.296	2.383
F(000)	2248.0	2344.0	2376.0
F000’	2235.29	2331.78	2363.76
Crystal size/mm^3	0.2 × 0.15 × 0.1	0.36×0.32 ×0.28	0.35 × 0.3 × 0.28
Radiation	Cu Kα (λ = 1.54184)	Cu Kα (λ = 1.54184)	Cu Kα (λ = 1.54184)
θ range	4.17 to 155.538	4.73 to 155.024	7.91 to 155.66
h,k,lmax	21,26,18	24,19,26	26,16,28
Index ranges	-21 ≤ h ≤ 19, -18 ≤ k ≤ 26, -18 ≤ l ≤ 18	-23 ≤ h ≤ 23, -19 ≤ k ≤ 16, -26 ≤ l ≤ 26	-23 ≤ h ≤ 25, -14 ≤ k ≤ 15, -28 ≤ l ≤ 28
Reflections collected	40915	40993	22161
Independent reflections	18584 [Rint = 0.0394, Rsigma = 0.0456]	12419 [Rint = 0.0668, Rsigma = 0.0444]	8038 [Rint = 0.0426, Rsigma = 0.0437]
Data/restraints/parameters	18584/2/1283	12419/0/676	8038/2/686
Goodness-of-fit on F^2	1.053	0.892	1.041
Data completeness	1.60/0.80	0.946	1.27/0.63
Theta(max)	77.769	77.512	77.830

Final *R* indexes [I>=2σ(*I*)]	R1 = 0.0495, wR2 = 0.1275	R1 = 0.1269, wR2 = 0.3153	R1 = 0.0508, wR2 = 0.1415
Final *R* indexes [all data]	R1 = 0.0530, wR2 = 0.1297	R1 = 0.1403, wR2 = 0.3264	R1 = 0.0521, wR2 = 0.1433
Largest diff. peak/hole/e Å^{-3}	0.90/-0.52	1.89/-1.62	1.39/-0.73
S	1.053	0.892	1.041
Npar	1283	676	686

5. ^{1}H,^{13}C and 2D NMR spectra of organic compounds

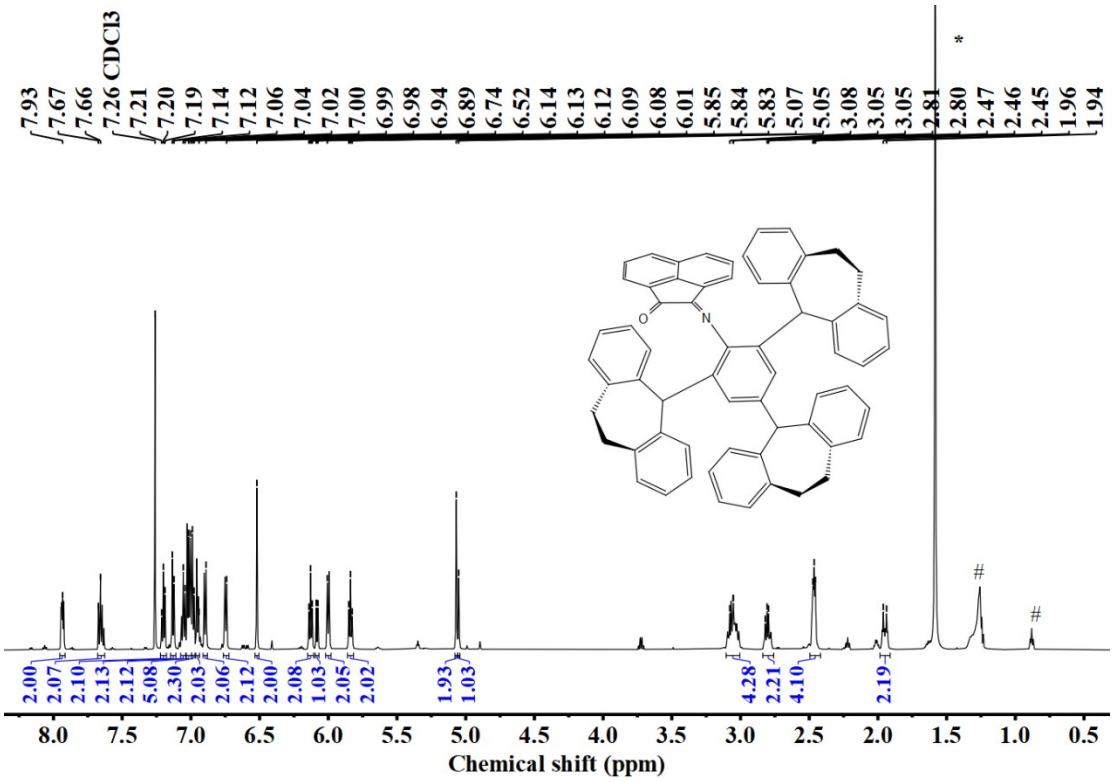

Figure S1. ^{1}H NMR spectra (in $CDCl_3$) of imino-ketone [* is water and # is hexane].

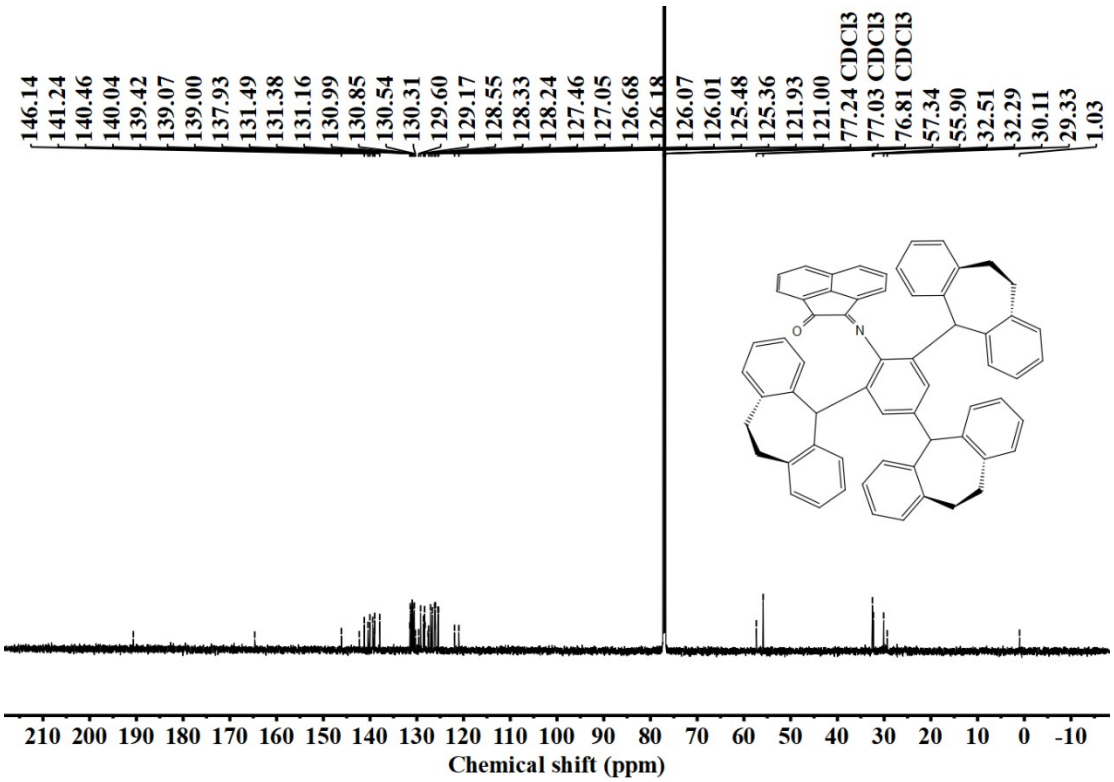

Figure S2. ^{13}C NMR spectra (in $CDCl_3$) of imino-ketone.

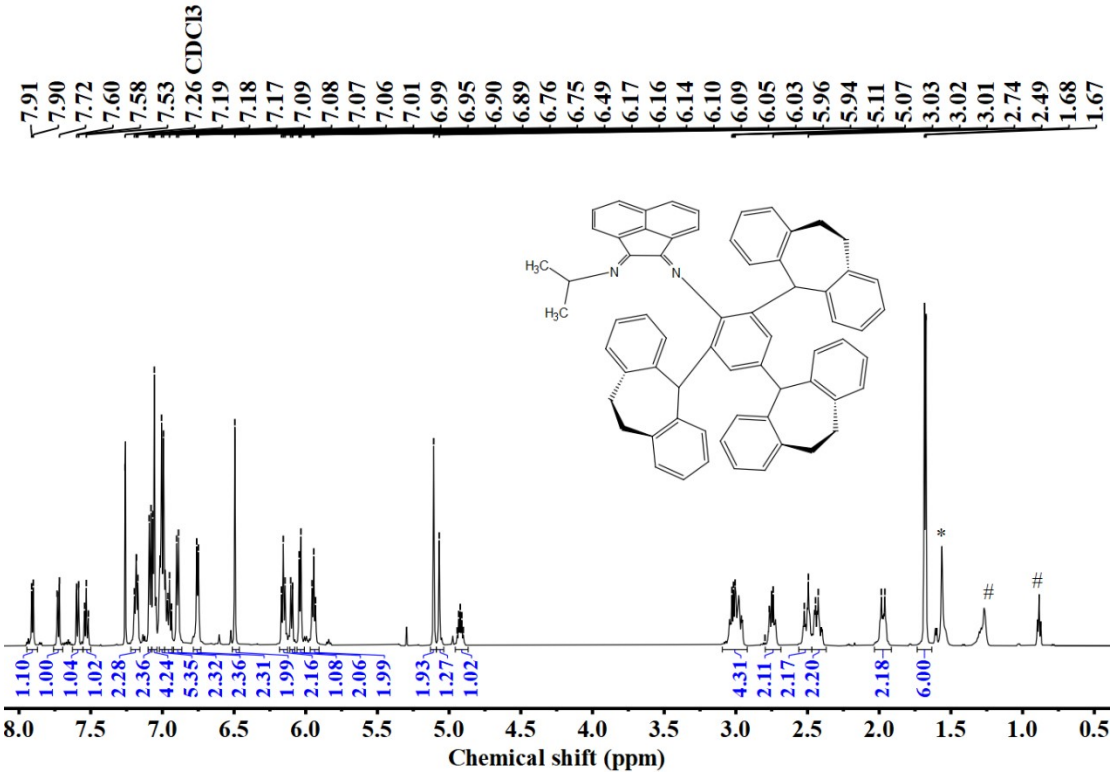

Figure S3. ^{1}H NMR spectra (in $CDCl_3$) of $\mathbf{L^{iPr}}$ [* is water and # is hexane].

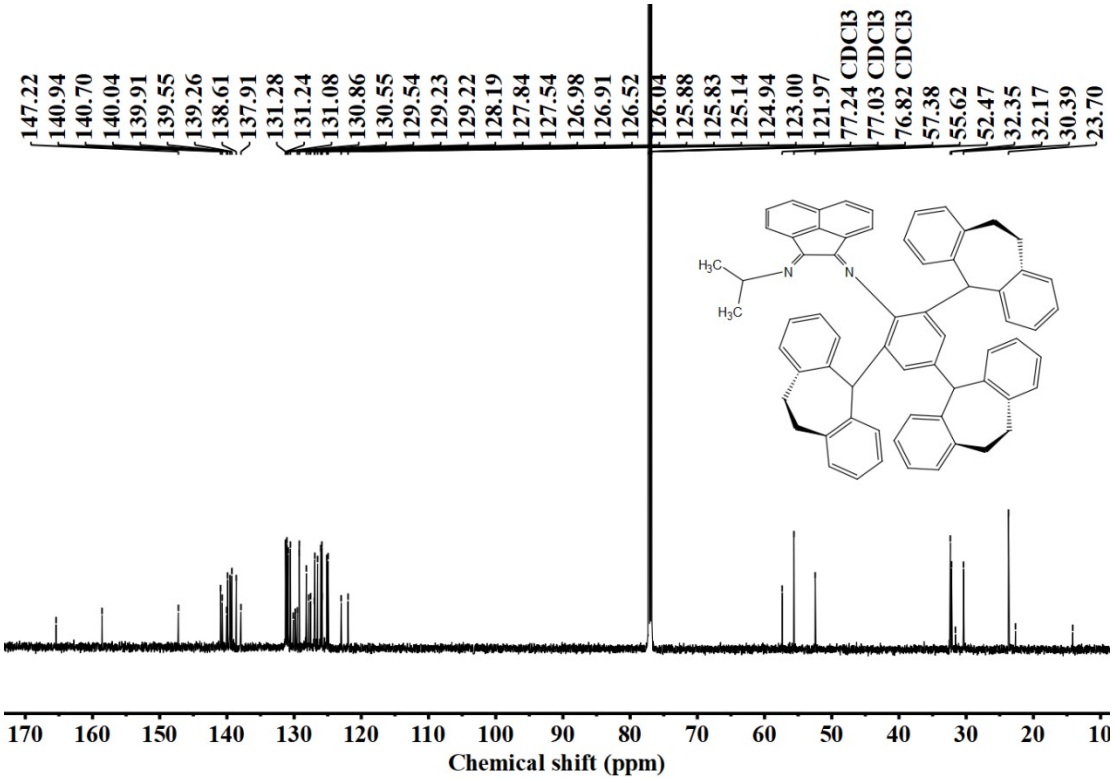

Figure S4. ^{13}C NMR spectra (in $CDCl_3$) of $\mathbf{L^{iPr}}$.

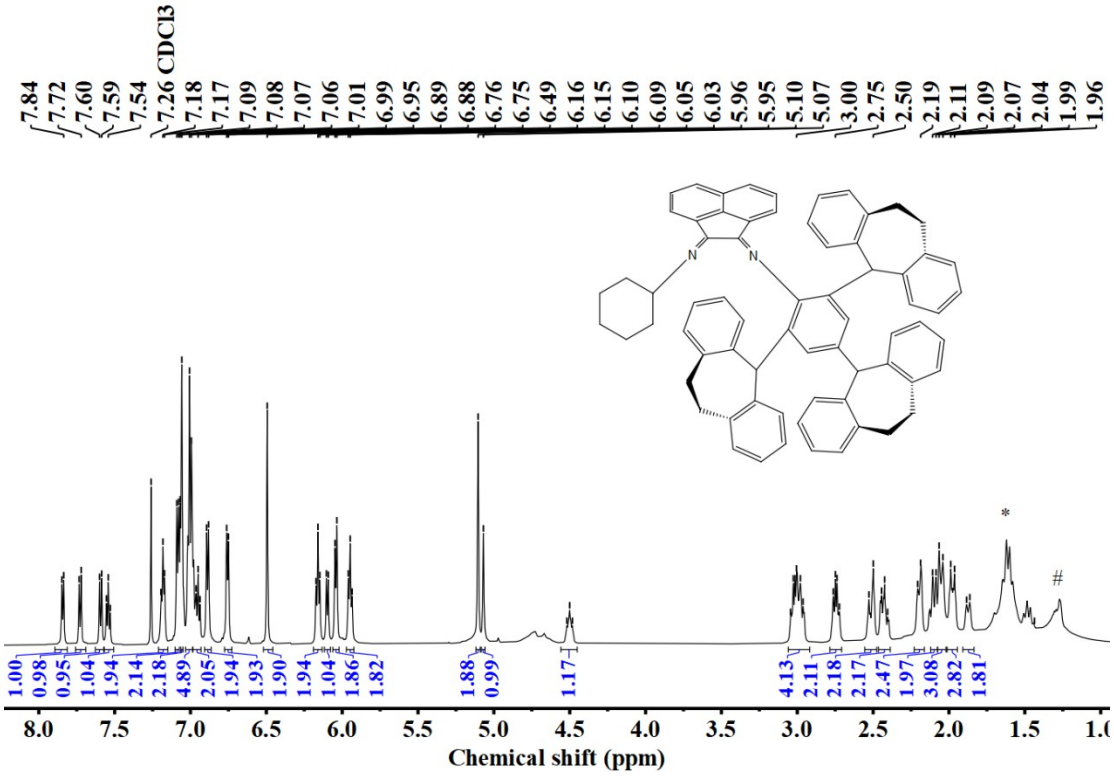

Figure S5. ^{1}H NMR spectra (in $CDCl_3$) of $\mathbf{L^{cH}}$ [* is water and # is hexane].

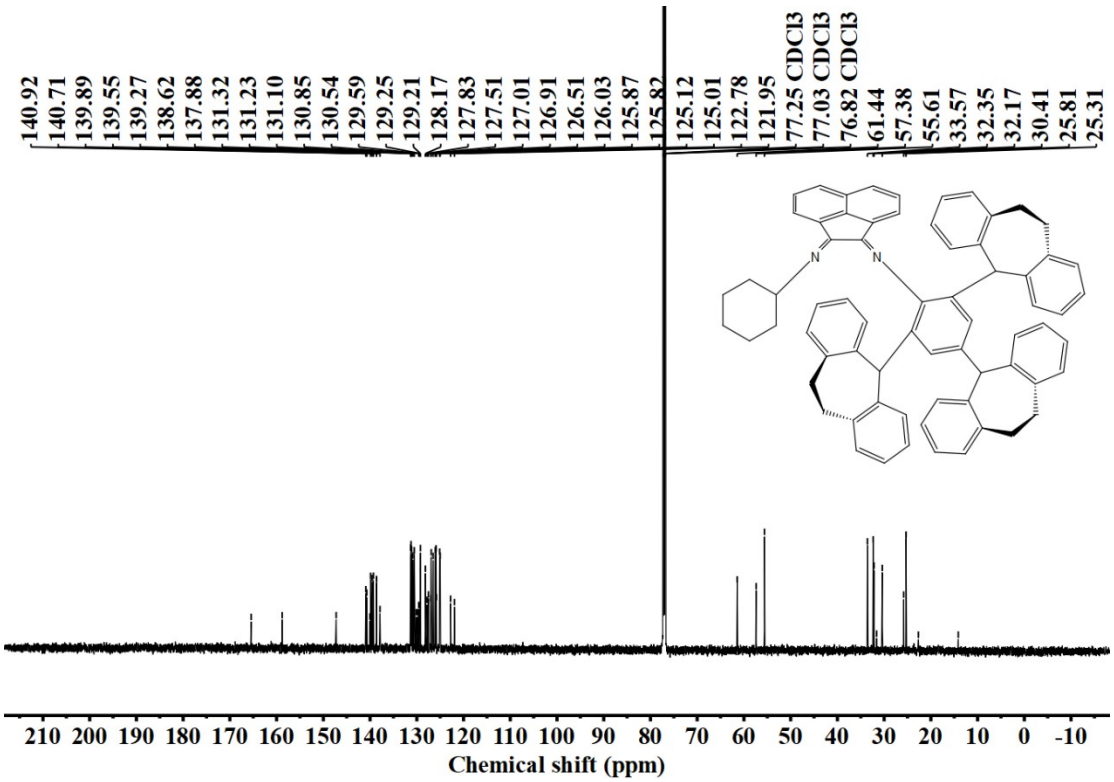

Figure S6. ^{13}C NMR spectra (in $CDCl_3$) of $\mathbf{L^{cH}}$.

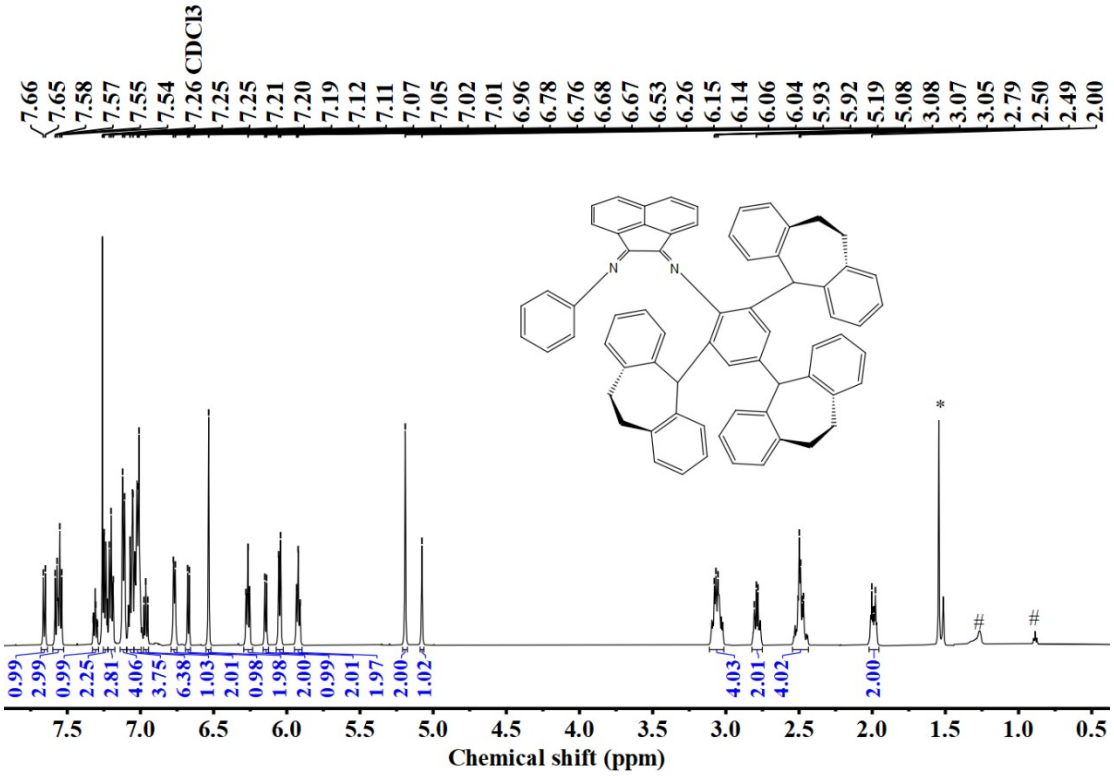

Figure S7. ^{1}H NMR spectra (in $CDCl_3$) of $\mathbf{L^{Ph}}$ [* is water and # is hexane].

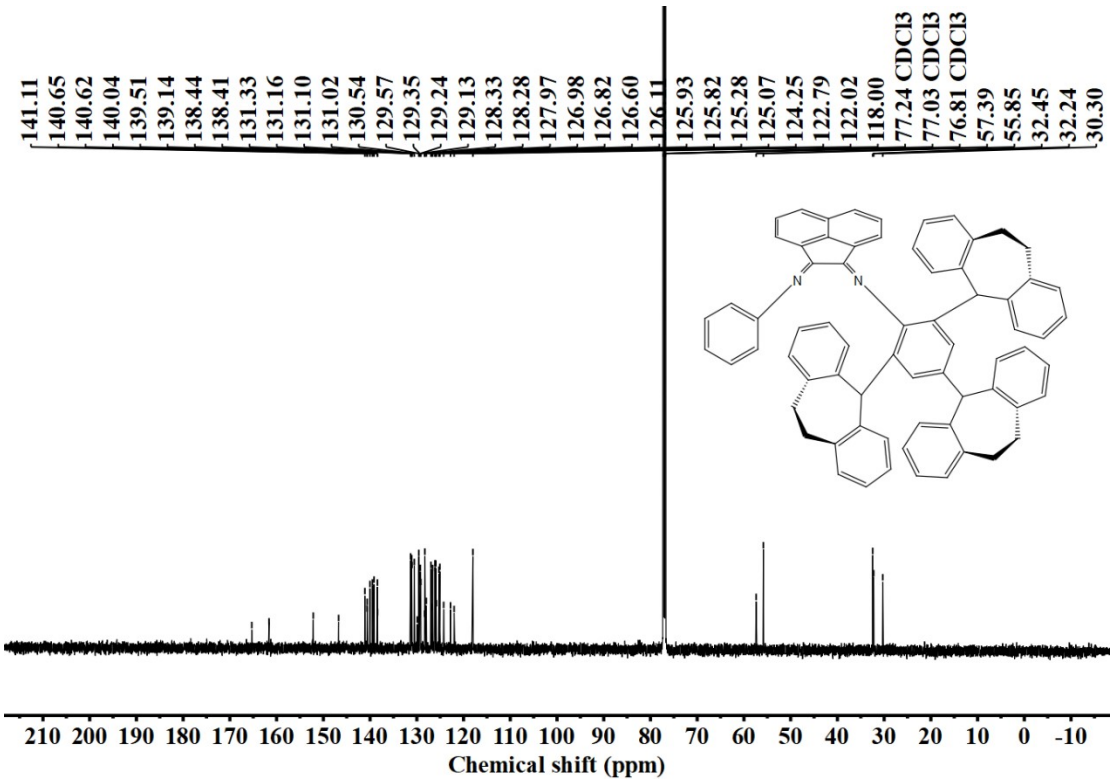

Figure S8. ^{13}C NMR spectra (in $CDCl_3$) of $\mathbf{L^{Ph}}$.

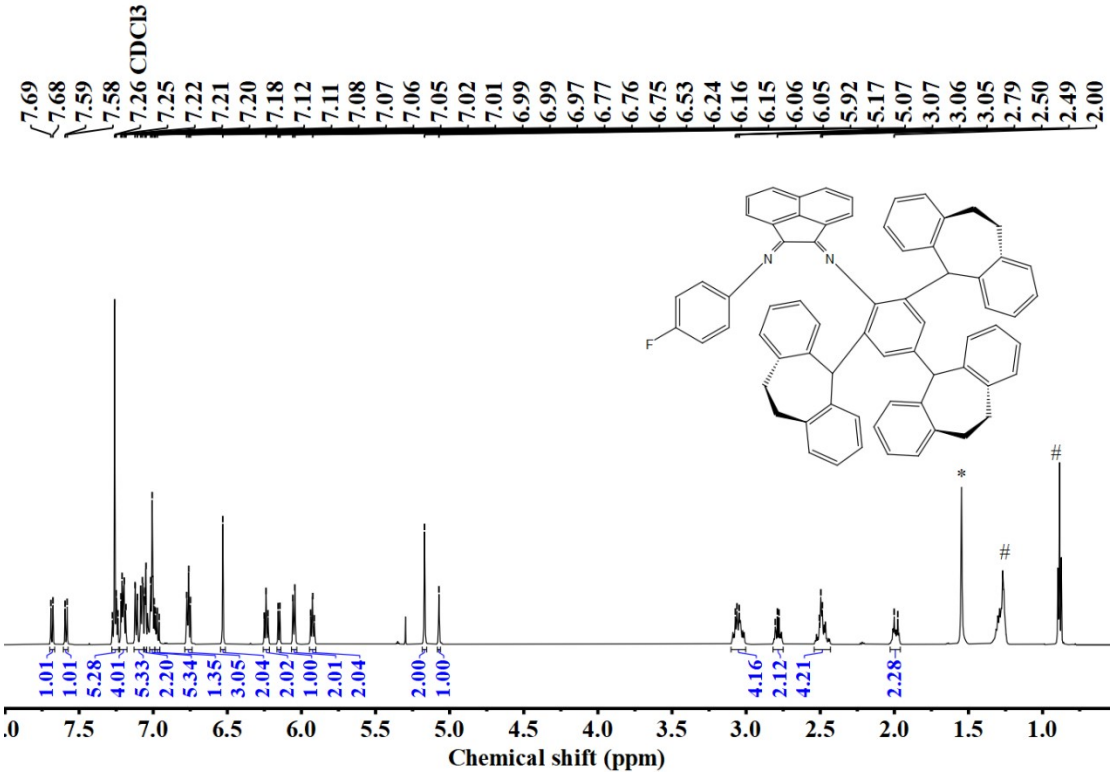

Figure S9. ^{1}H NMR spectra (in $CDCl_3$) of $\mathbf{L^{PhF}}$ [* is water and # is hexane].

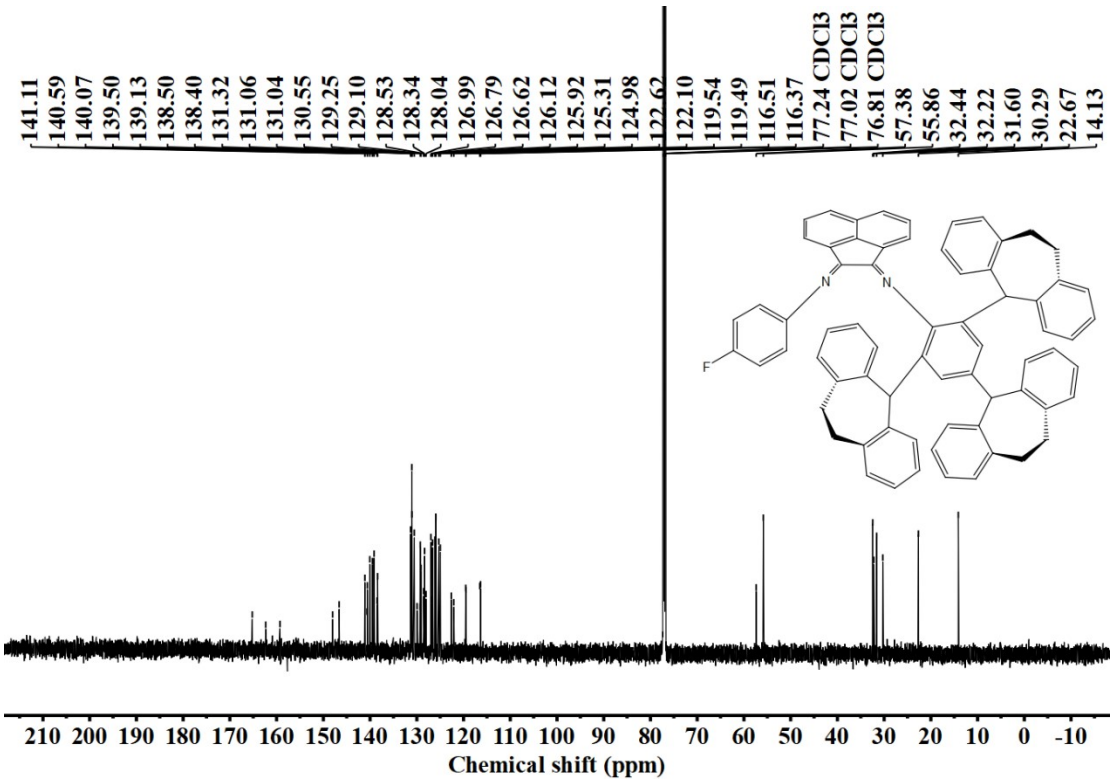

Figure S10. ^{13}C NMR spectra (in $CDCl_3$) of $\mathbf{L^{PhF}}$.

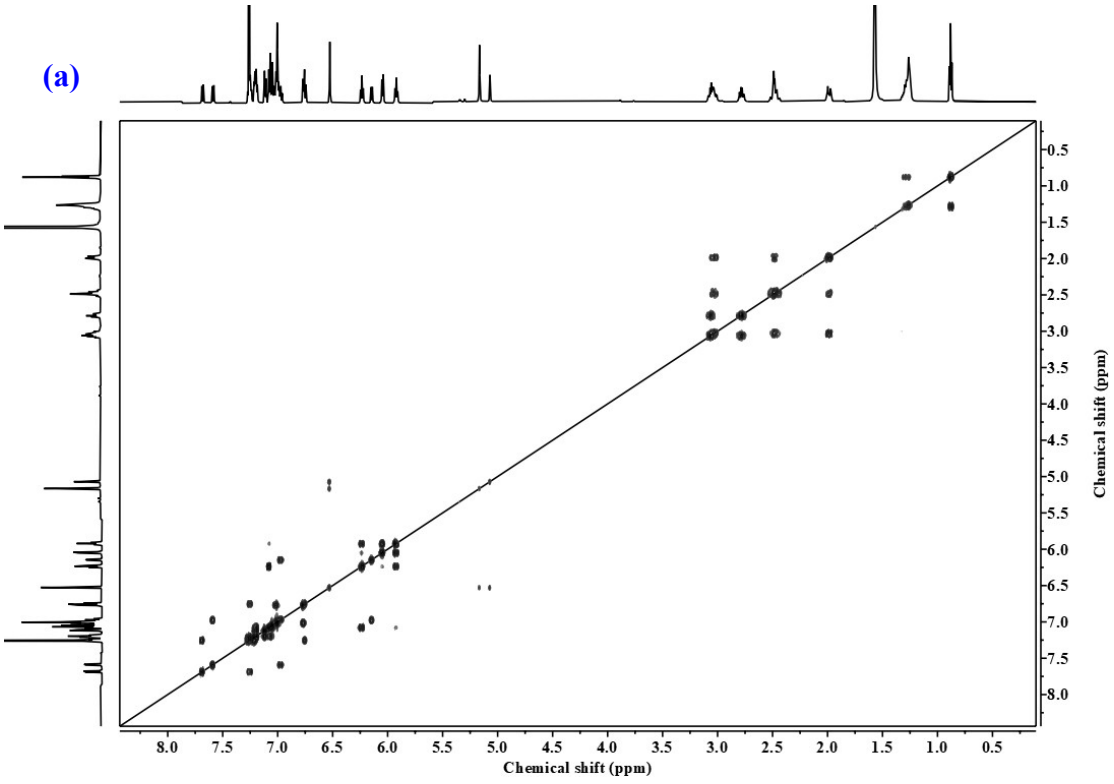

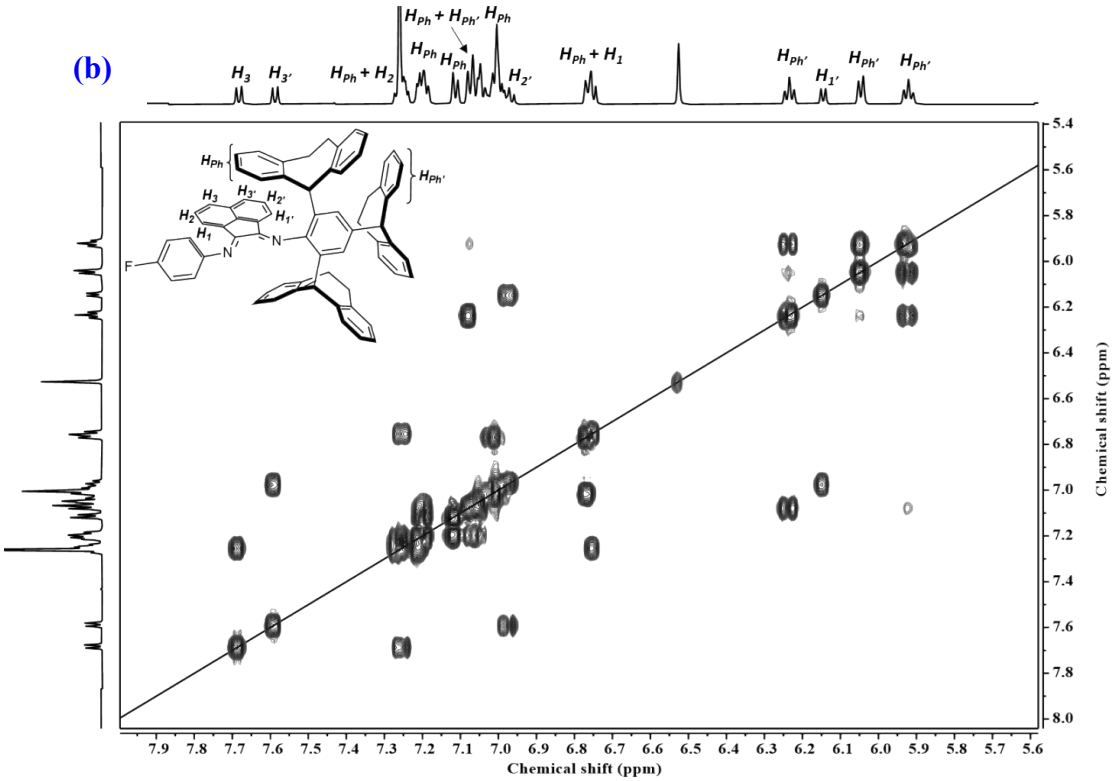

Figure S11. (a) ^{1}H-^{1}H 2D COSY NMR spectra (in $CDCl_3$) of $\mathbf{L^{PhF}}$; (b) ^{1}H-^{1}H 2D COSY NMR spectrum of $\mathbf{L^{PhF}}$ in $CDCl_3$ (from chemical shift 5.6 - 7.9 ppm).

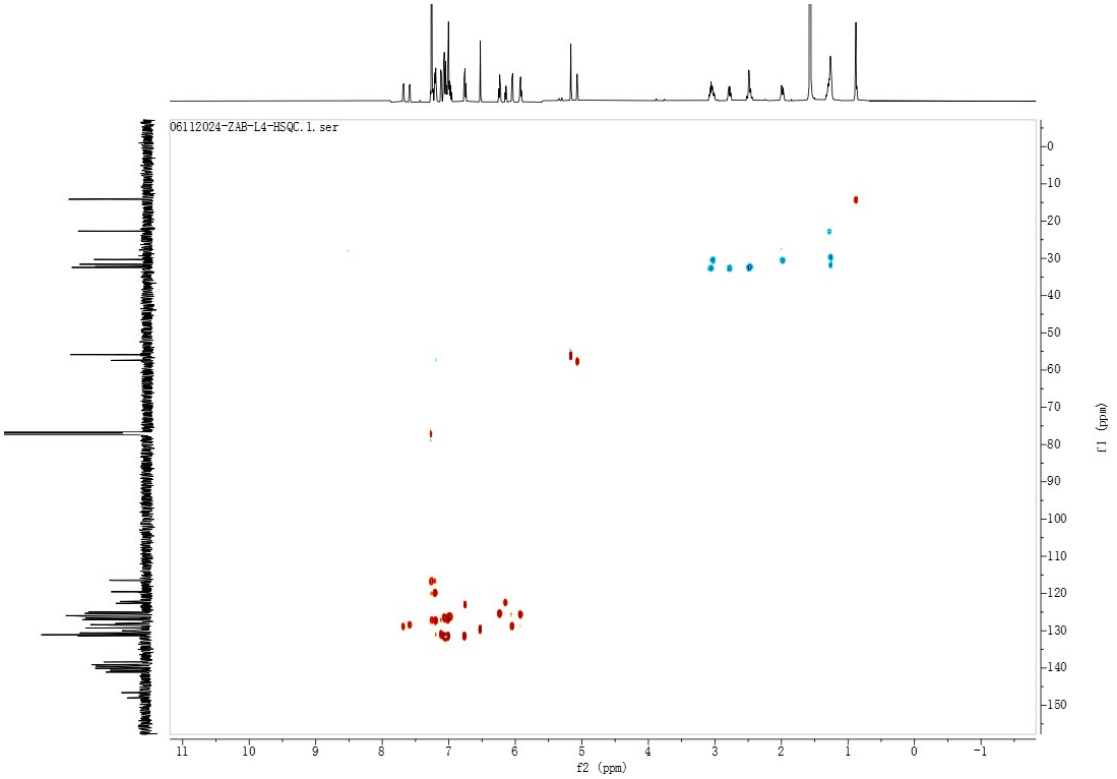

Figure S12. 2D HSQC NMR spectra (in $CDCl_3$) of $\mathbf{L^{PhF}}$

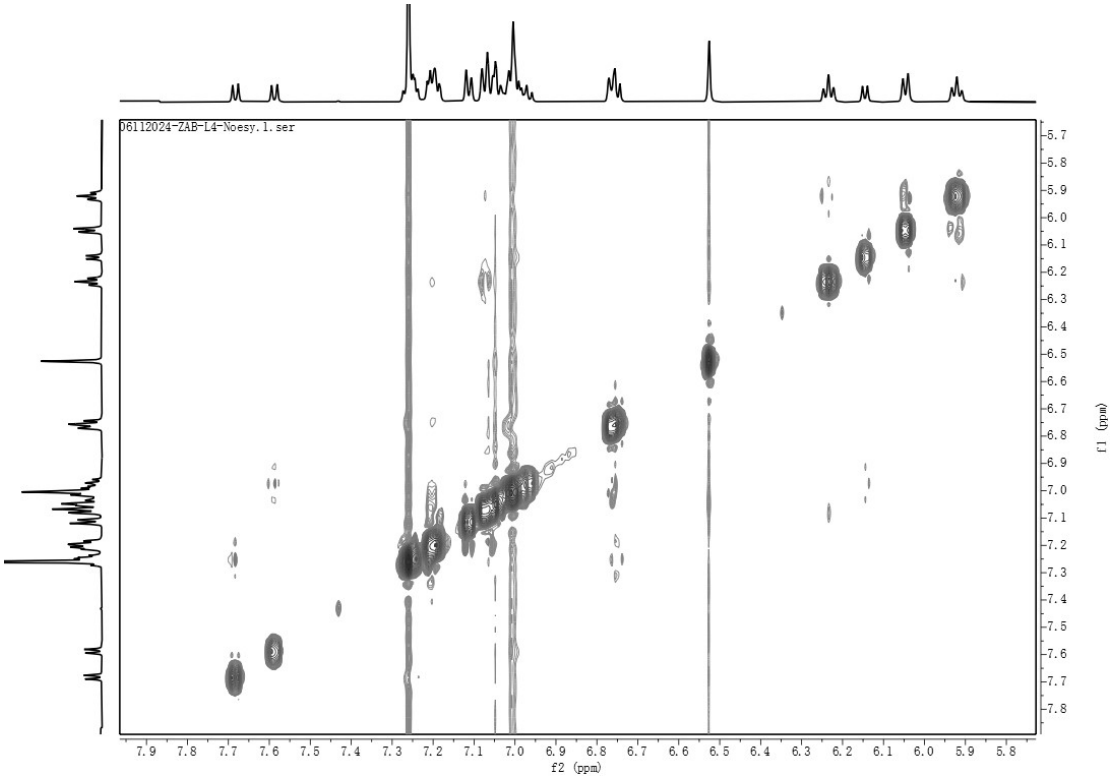

Figure S13. ^{1}H-^{1}H 2D NOESY NMR spectra (in $CDCl_3$) of $\mathbf{L^{PhF}}$

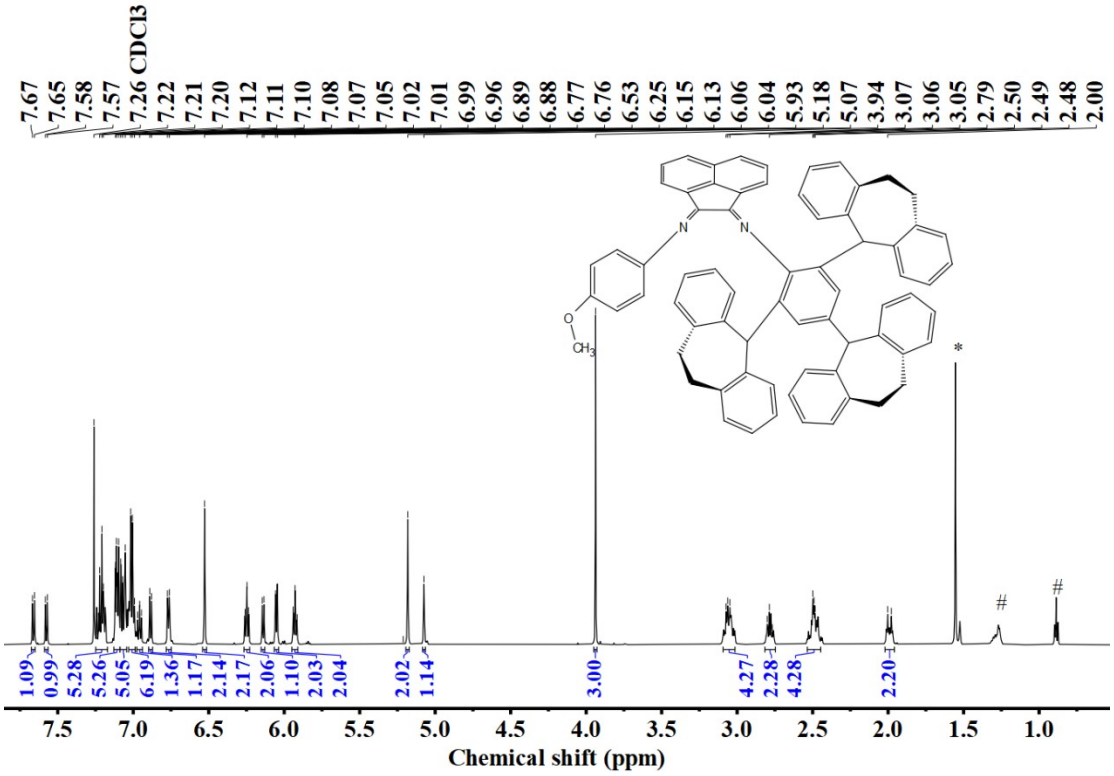

Figure S14. ^{1}H NMR spectra (in $CDCl_3$) of $\mathbf{L^{PhOMe}}$ [* is water and # is hexane].

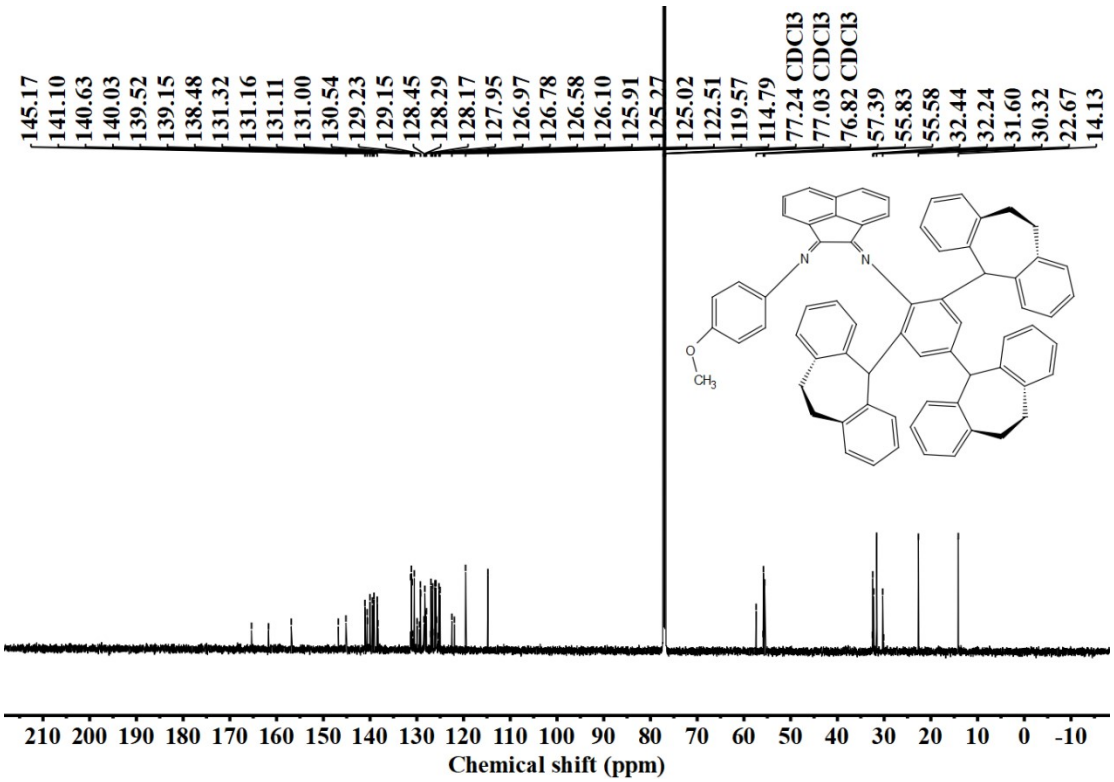

Figure S15. ^{13}C NMR spectra (in $CDCl_3$) of $\mathbf{L^{PhOMe}}$.

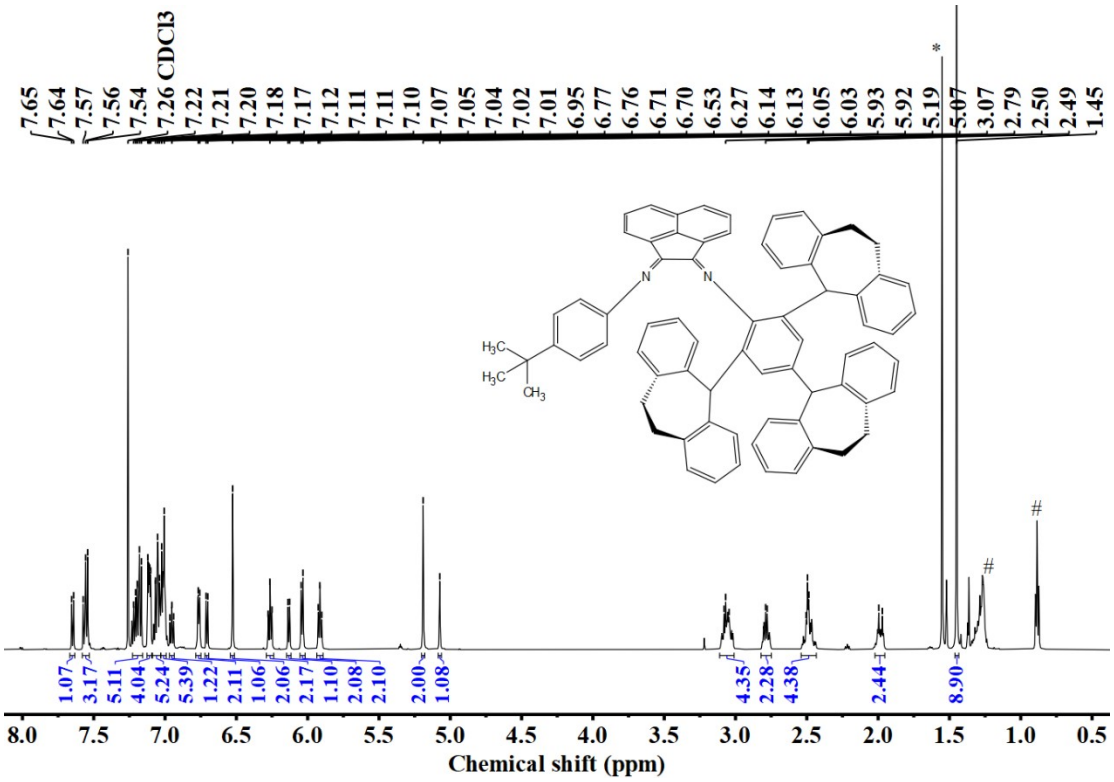

Figure S16. ^{1}H NMR spectra (in $CDCl_3$) of $\mathbf{L^{PhtBu}}$ [* is water and # is hexane].

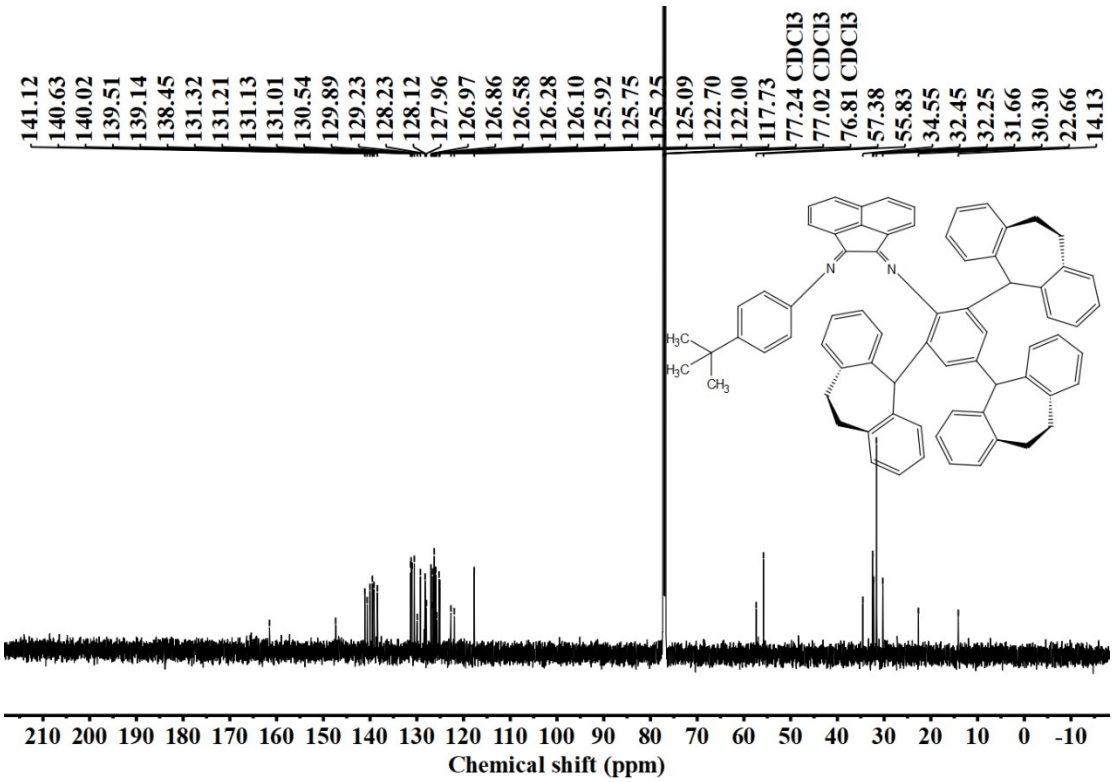

Figure S17. ^{13}C NMR spectra (in $CDCl_3$) of $\mathbf{L^{PhtBu}}$.

6. ^{1}H NMR spectra of obtained polyethylene using different nickel complexes at different temperatures.

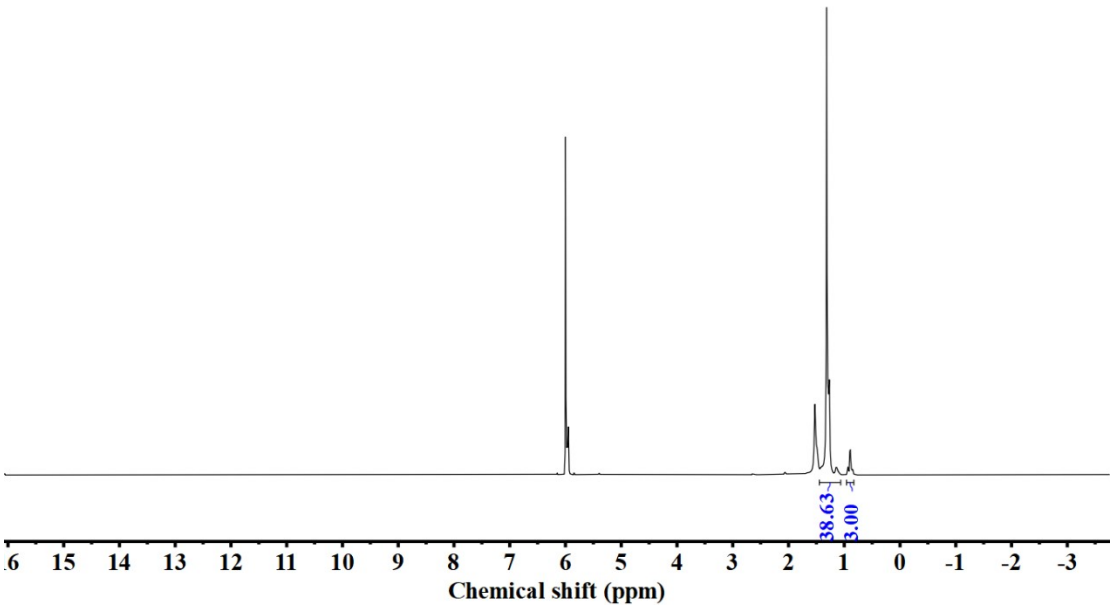

Figure S18. ^{1}H NMR spectra of polyethylene produced using $\mathbf{Ni^{Ph}/EASC}$ at 30 °C (entry 3, Table 3).

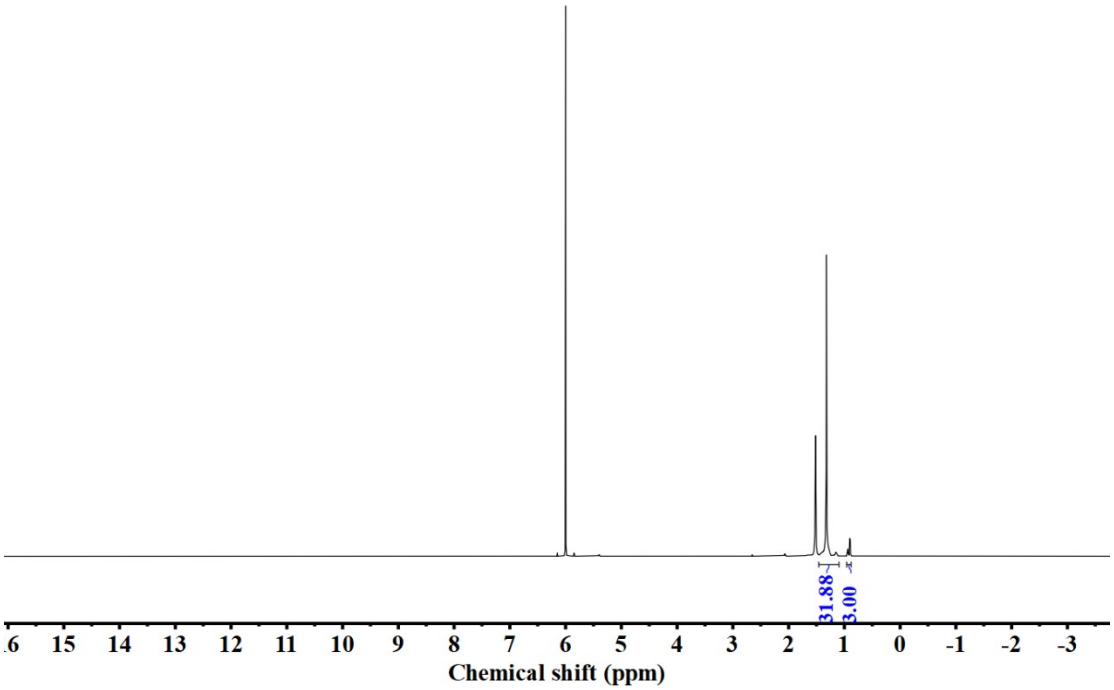

Figure S19. ^{1}H NMR spectra of polyethylene produced using **Ni^{Ph}/EASC** at 40 °C (entry 4, Table 3).

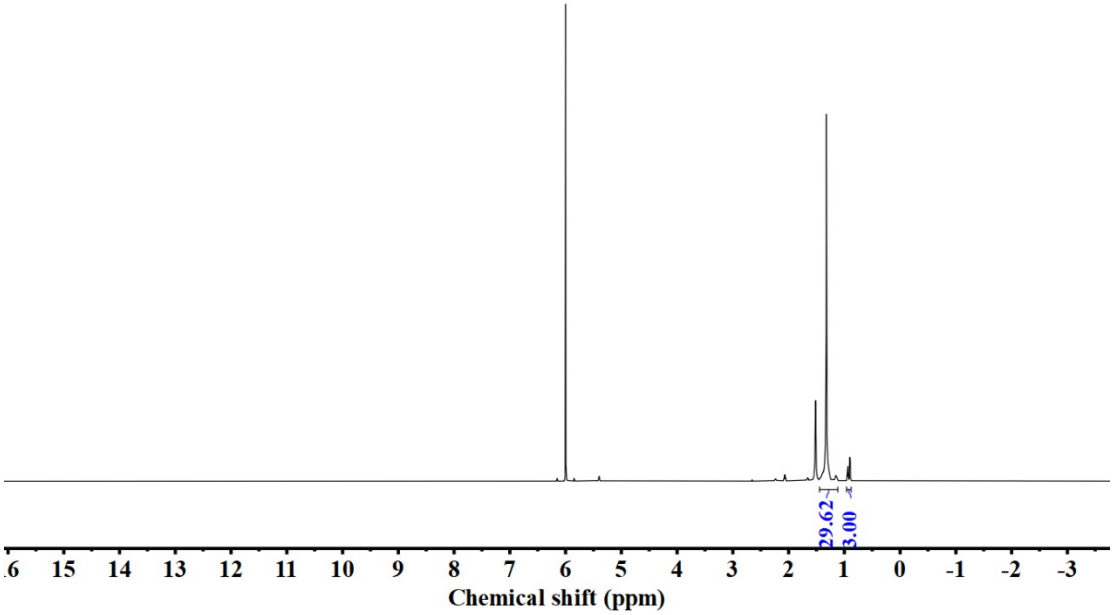

Figure S20. ^{1}H NMR spectra of polyethylene produced using **Ni^{Ph}/EASC** at 60 °C (entry 5, Table 3).

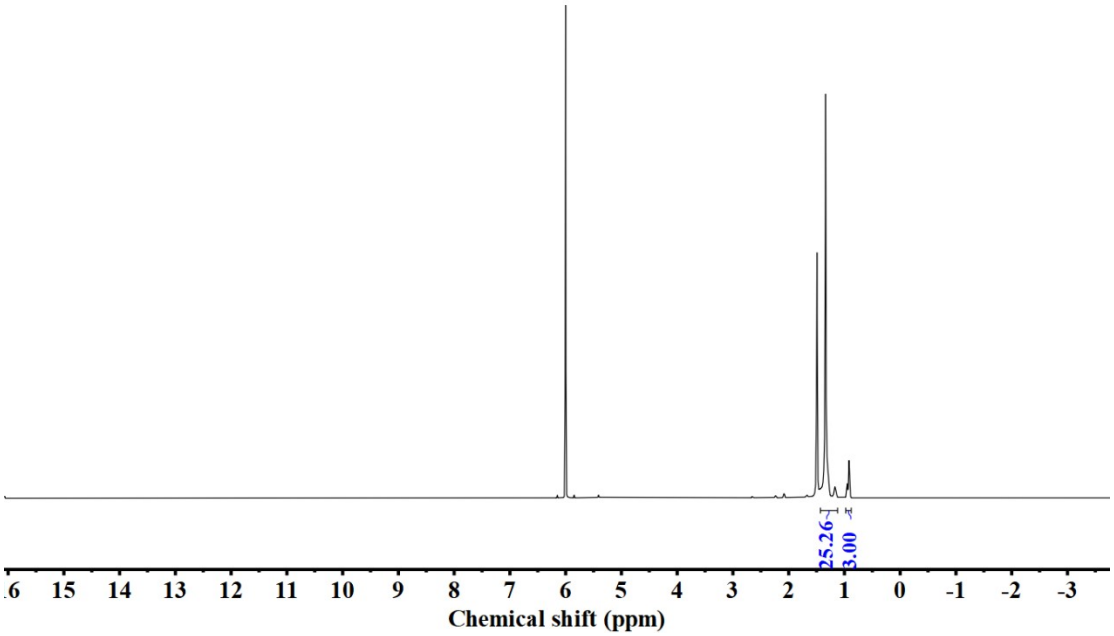

Figure S21. ^{1}H NMR spectra of polyethylene produced using **Ni^{Ph}/EASC** at 80 °C (entry 6, Table 3).

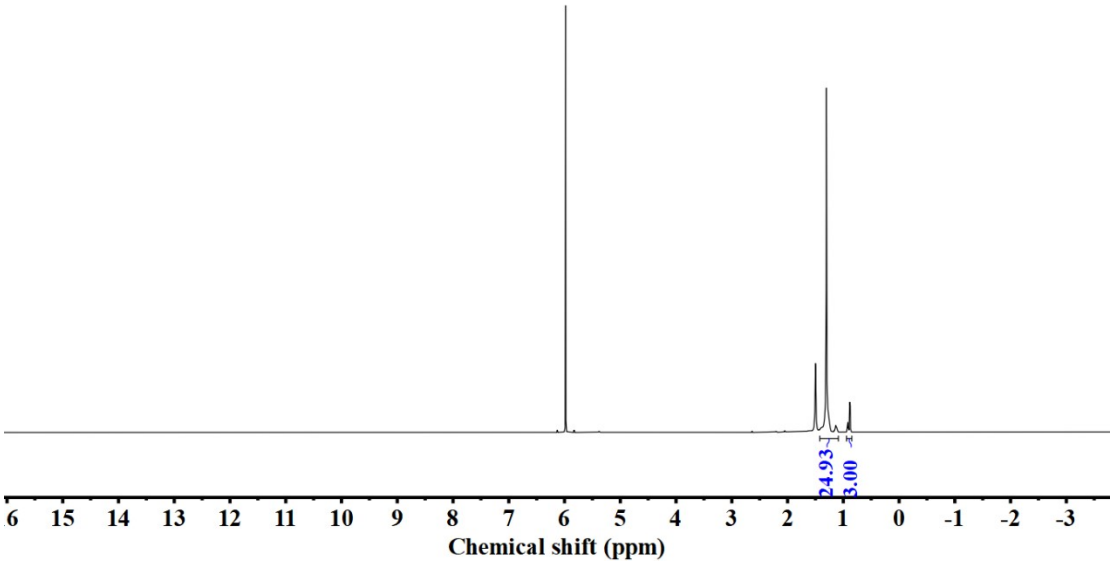

Figure S22. ^{1}H NMR spectra of polyethylene produced using **Ni^{Ph}/EASC** at 100 °C (entry 7, Table 3).

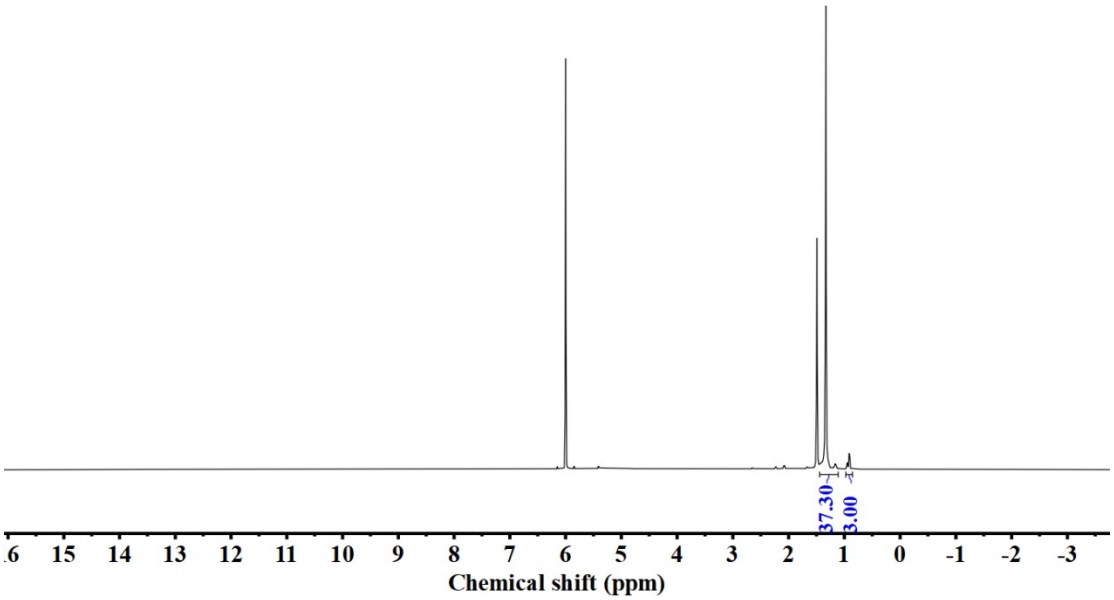

Figure S23. ^{1}H NMR spectra of polyethylene produced using **Ni^{PhF}/EASC** at 30 °C (entry 8, Table 3).

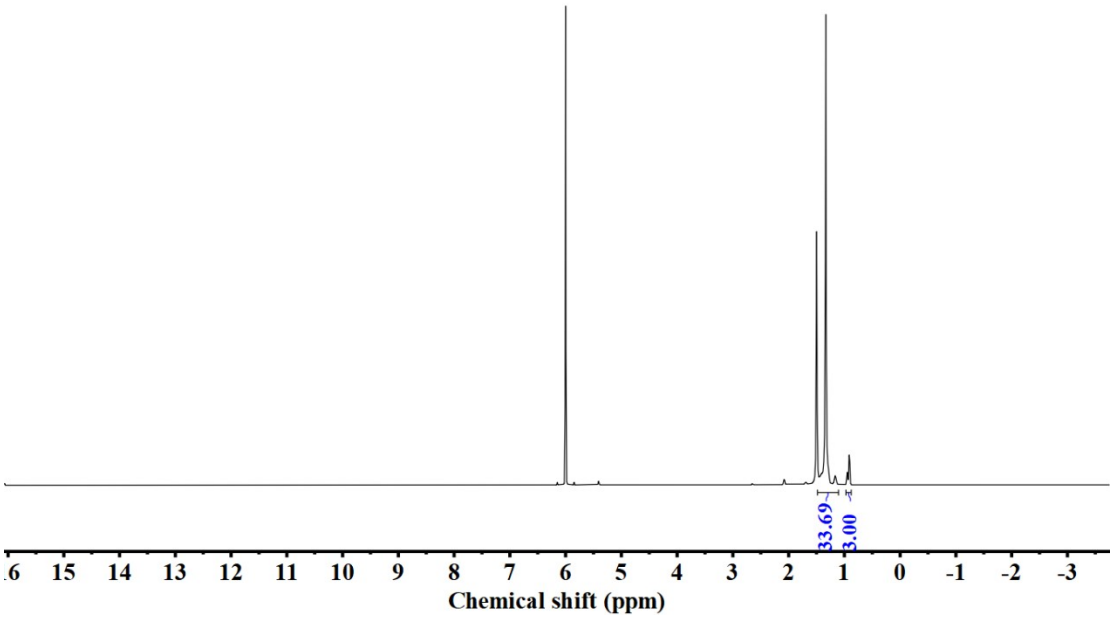

Figure S24. ^{1}H NMR spectra of polyethylene produced using **Ni^{PhF}/EASC** at 40 °C (entry 9, Table 3).

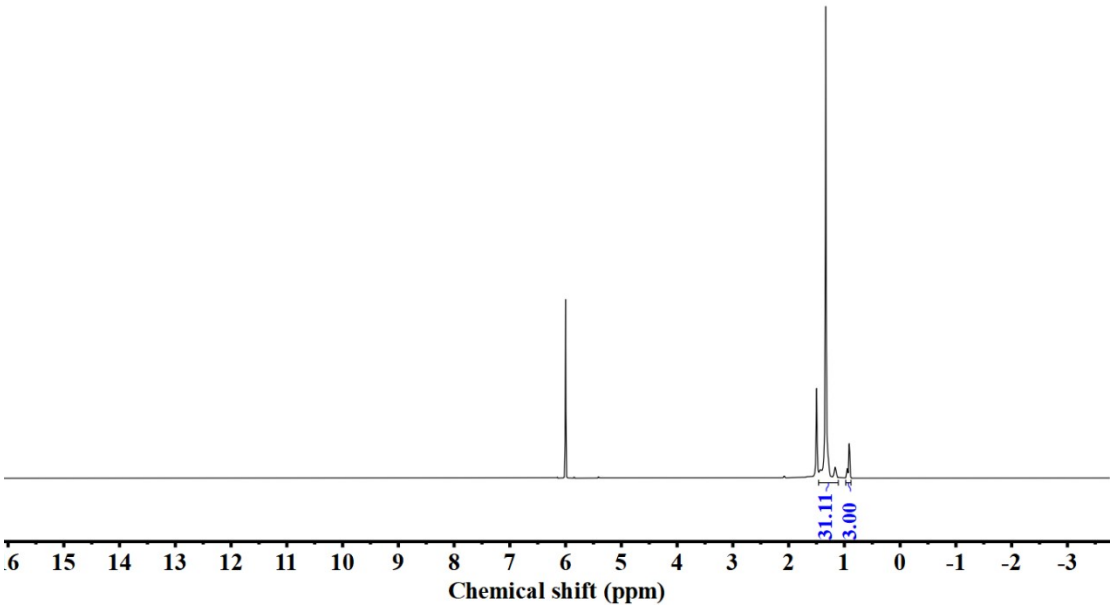

Figure S25. ^{1}H NMR spectra of polyethylene produced using **Ni^{PhF}/EASC** at 60 °C (entry 10, Table 3).

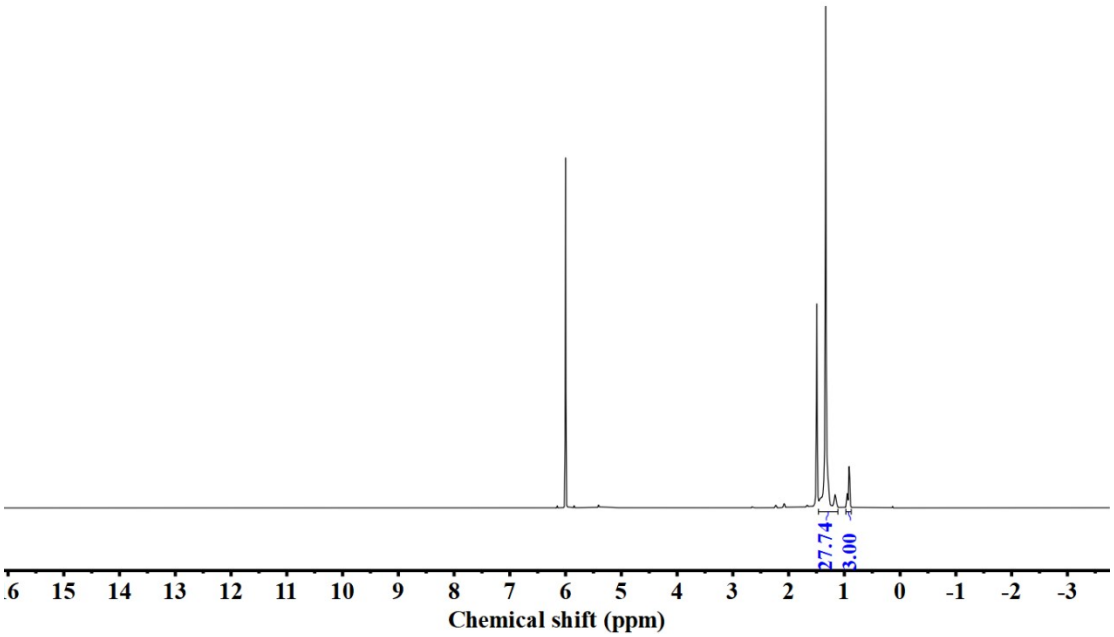

Figure S26. ^{1}H NMR spectra of polyethylene produced using **Ni^{PhF}/EASC** at 80 °C (entry 11, Table 3).

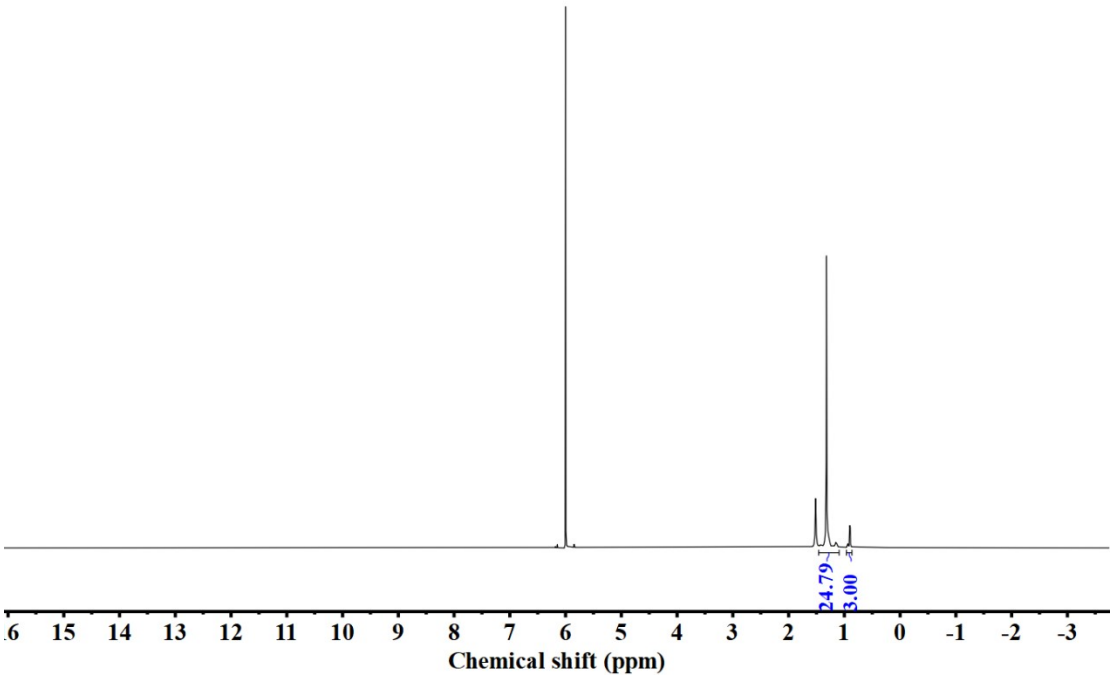

Figure S27. ^{1}H NMR spectra of polyethylene produced using **Ni^{PhF}/EASC** at 100 °C (entry 12, Table 3).

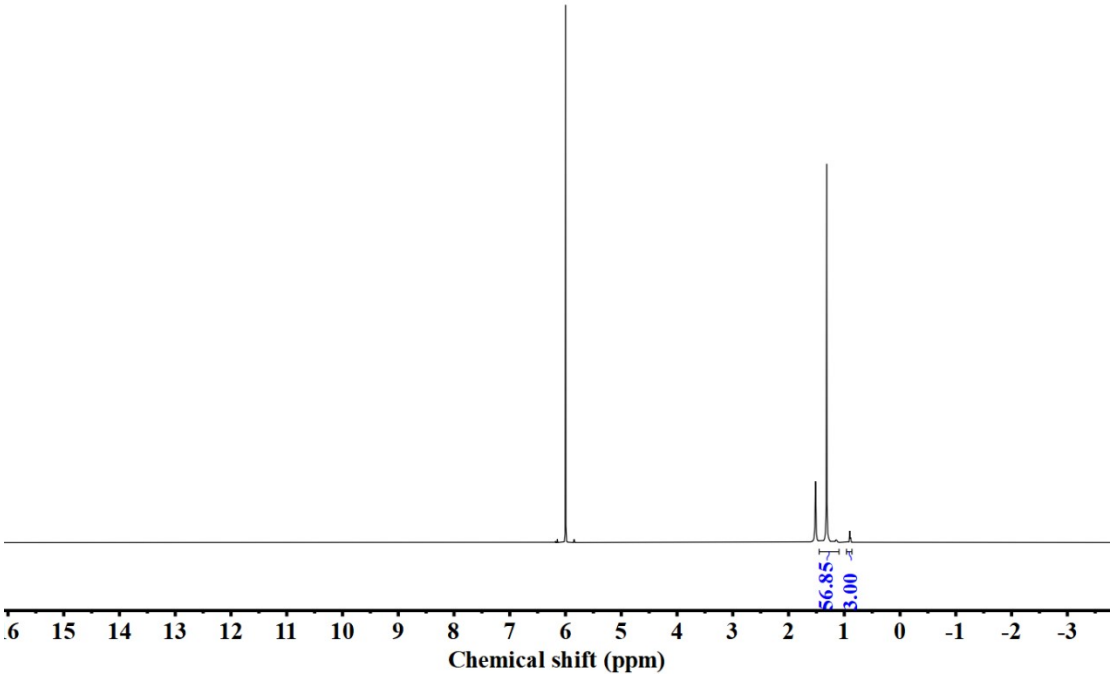

Figure S28. ^{1}H NMR spectra of polyethylene produced using **Ni^{PhOMe}/EASC** at 30 °C (entry 13, Table 3).

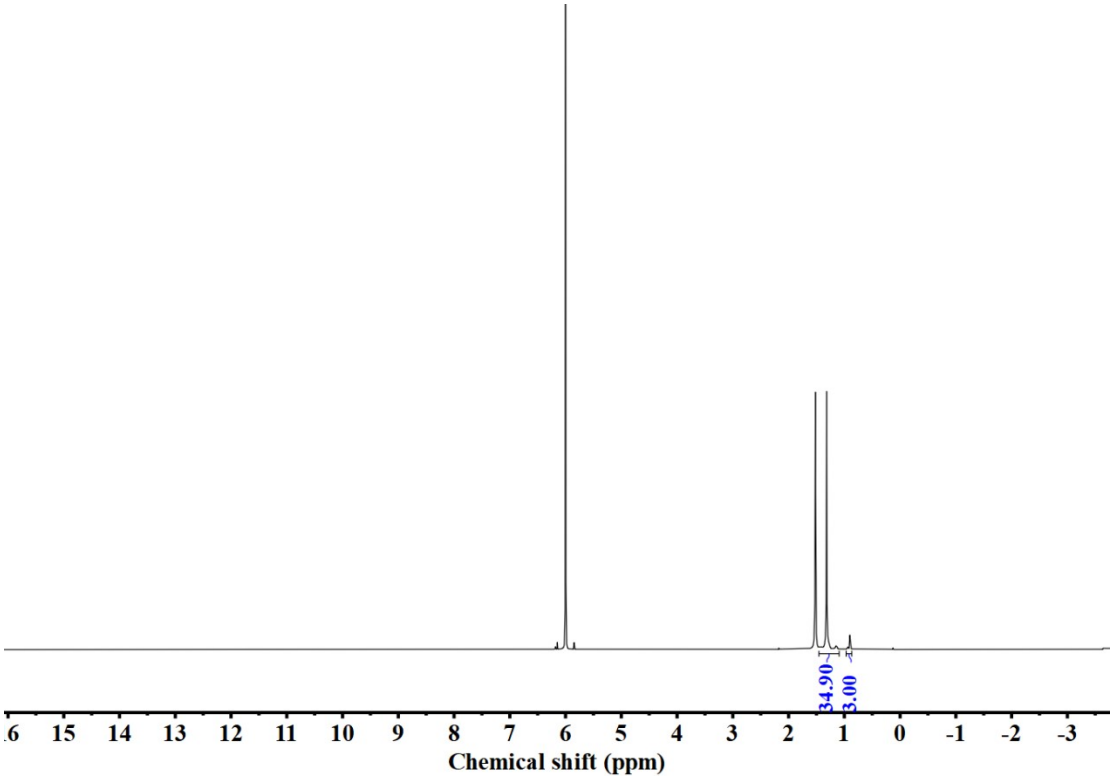

Figure S29. ^{1}H NMR spectra of polyethylene produced using **Ni^{PhOMe}/EASC** at 40 °C (entry 14, Table 3).

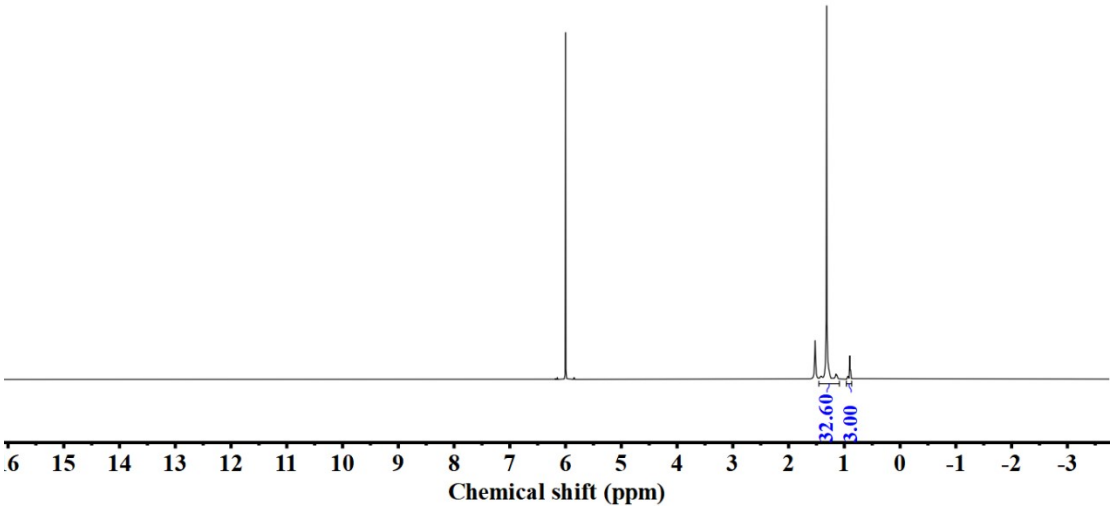

Figure S30. ^{1}H NMR spectra of polyethylene produced using **Ni^{PhOMe}/EASC** at 60 °C (entry 15, Table 3).

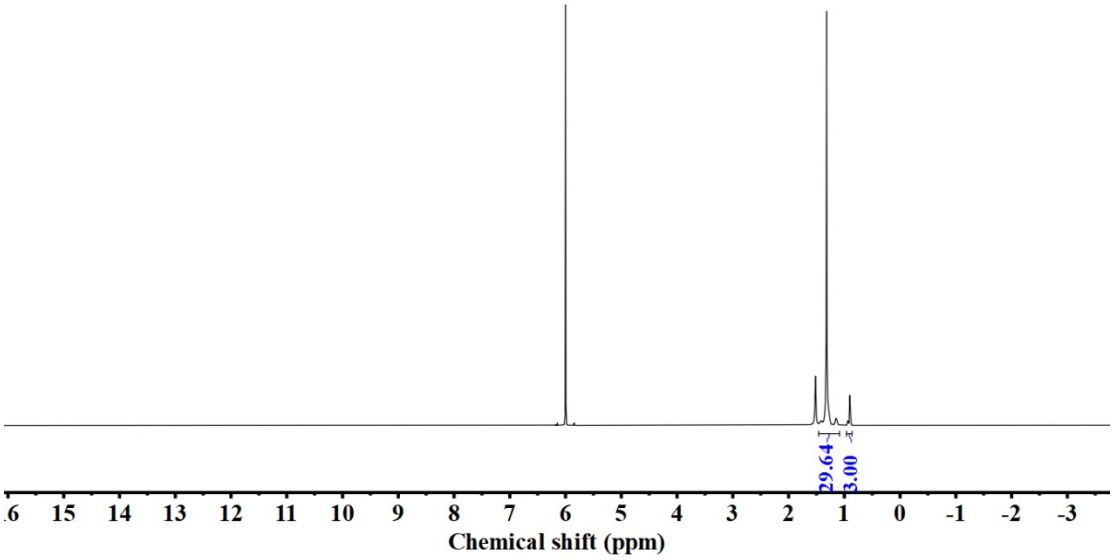

Figure S31. ^{1}H NMR spectra of polyethylene produced using **Ni^{PhOMe}/EASC** at 80 °C (entry 16, Table 3).

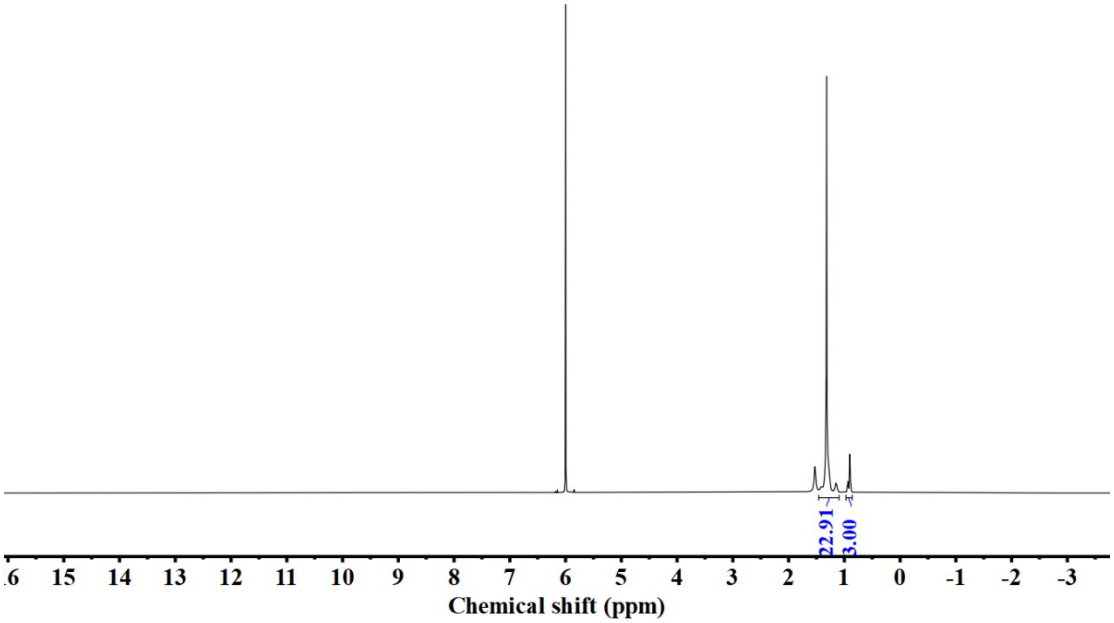

Figure S32. ^{1}H NMR spectra of polyethylene produced using **Ni^{PhOMe}/EASC** at 100 °C (entry 17, Table 3).

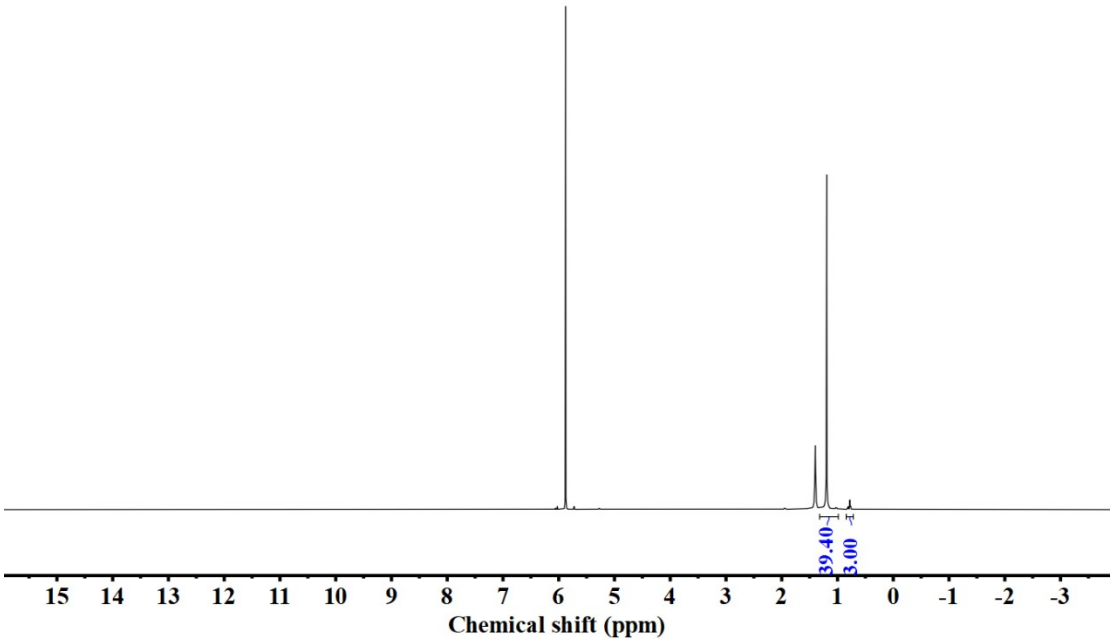

Figure S33. ^{1}H NMR spectra of polyethylene produced using **Ni^{PhtBu}/EASC** at 30 °C (entry 18, Table 3).

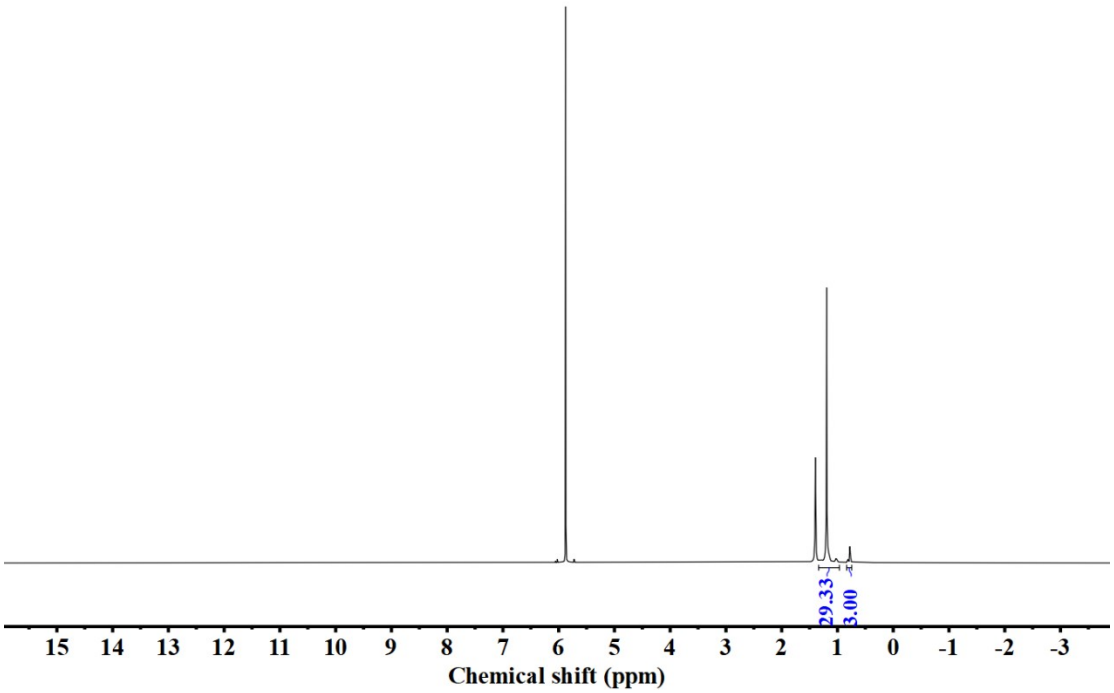

Figure S34. ^{1}H NMR spectra of polyethylene produced using **Ni^{PhtBu}/EASC** at 40 °C (entry 19, Table 3).

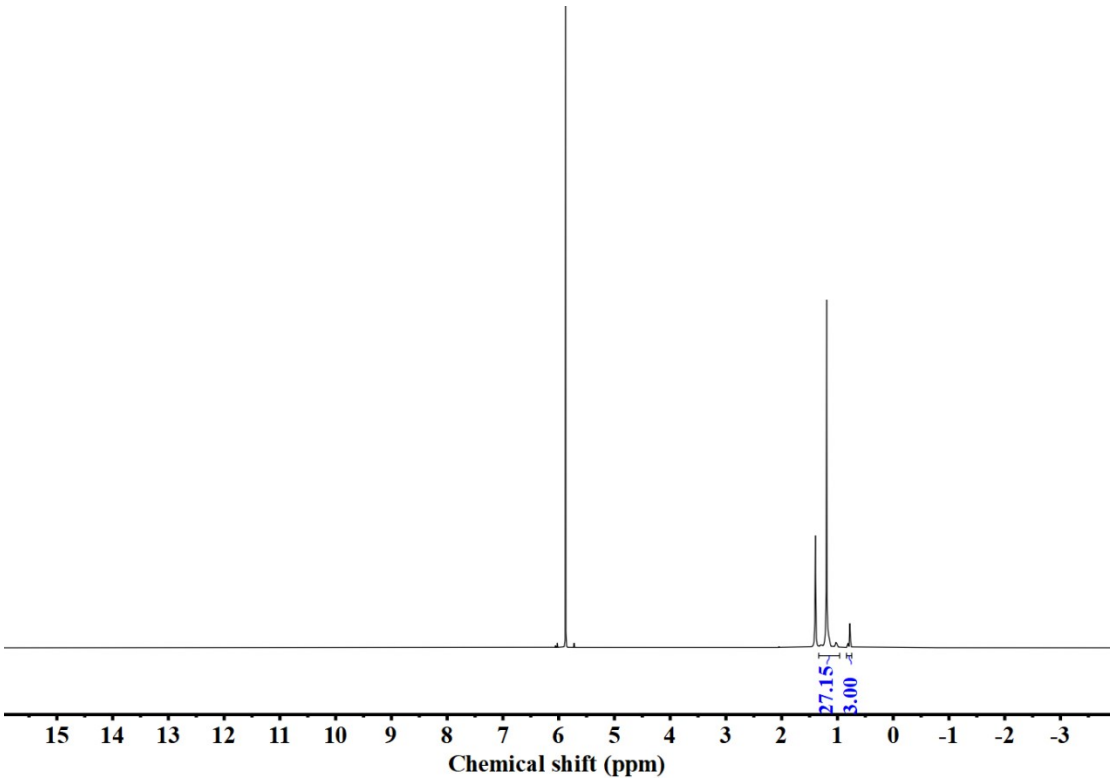

Figure S35. ^{1}H NMR spectra of polyethylene produced using **Ni^{PhtBu}/EASC** at 60 °C (entry 20, Table 3).

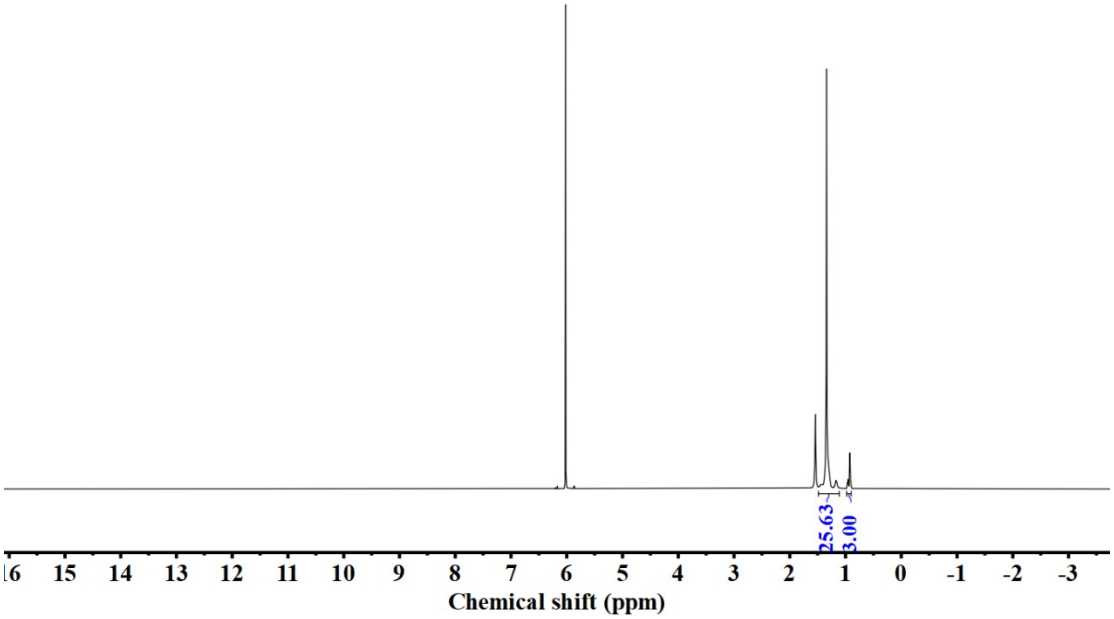

Figure S36. ^{1}H NMR spectra of polyethylene produced using **Ni^{PhtBu}/EASC** at 80 °C (entry 21, Table 3).

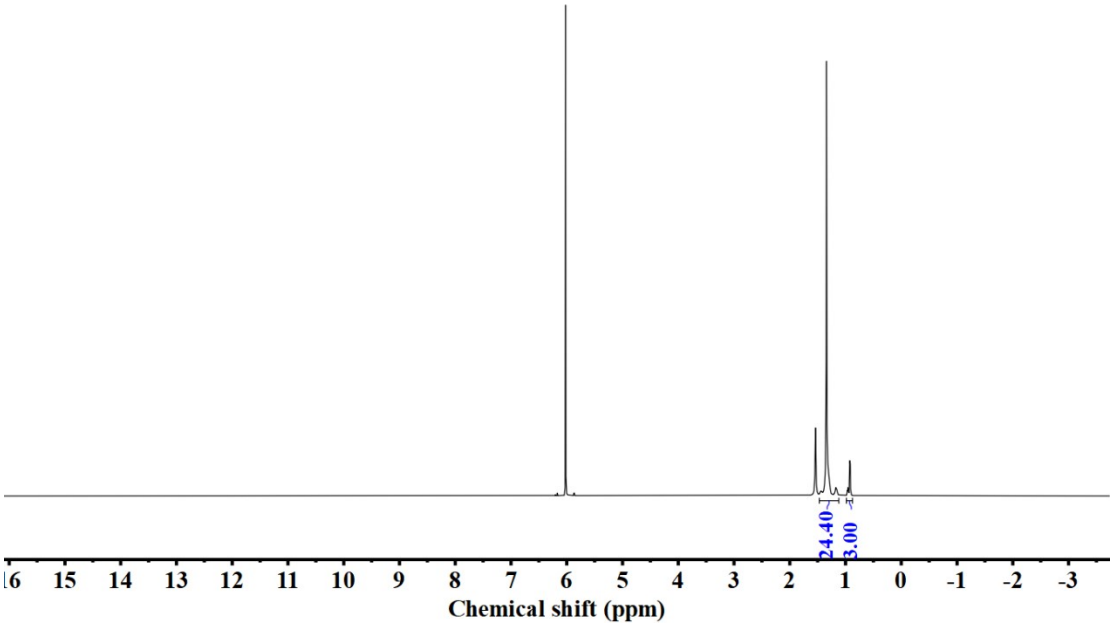

Figure S37. ^{1}H NMR spectra of polyethylene produced using **Ni^{PhtBu}/EASC** at 100 °C (entry 22, Table 3).

7. ^{13}C NMR spectrum of polyethylene obtained at different polymerization temperature using Ni^{OMe}

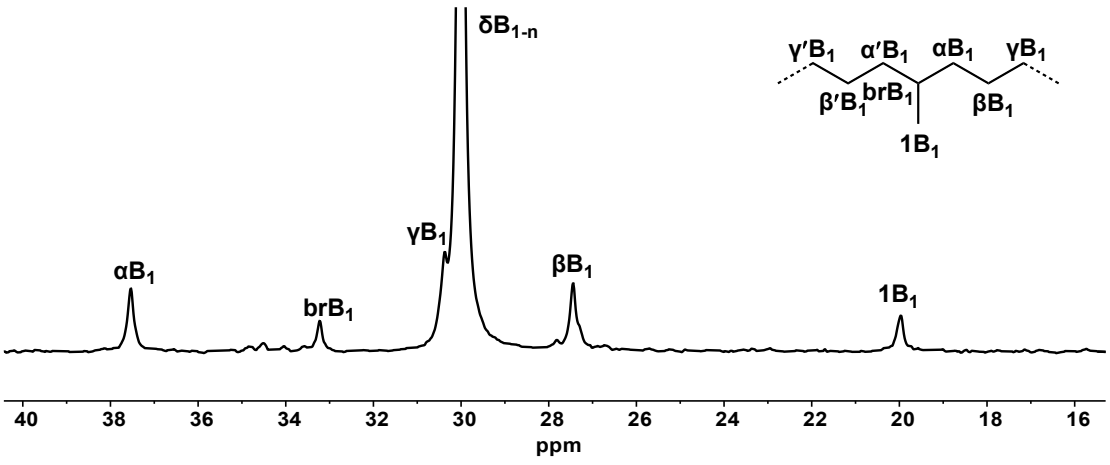

Figure S38. ^{13}C NMR spectrum of polyethylene obtained at polymerization temperature of 30 °C using **Ni^{OMe}** (entry 13, Table 3).

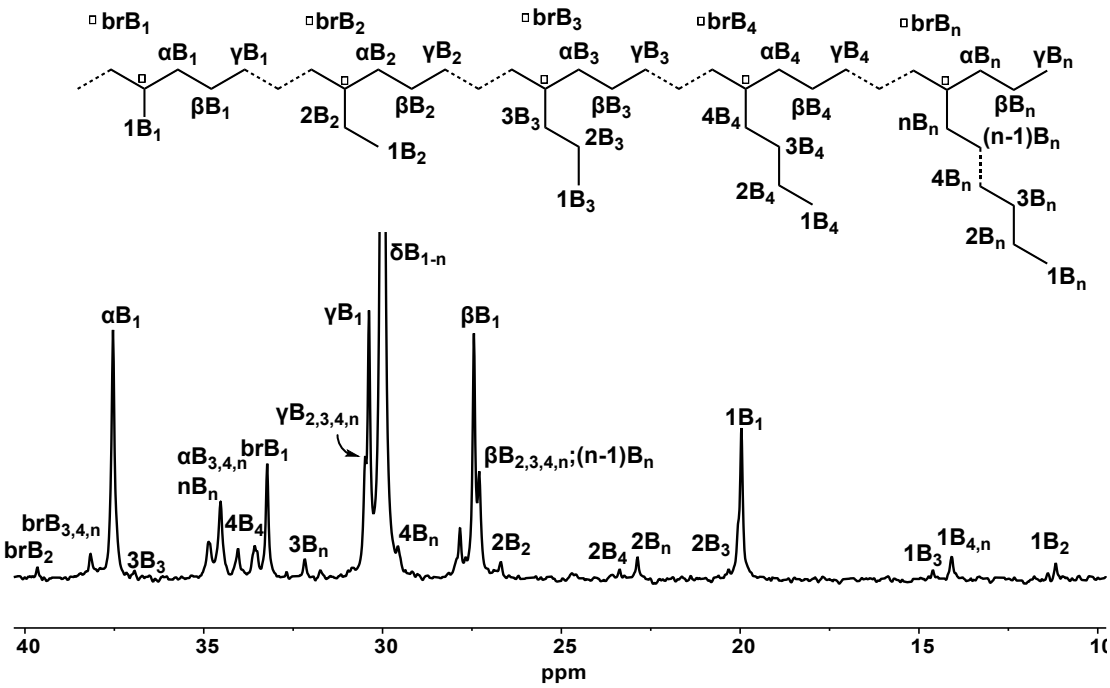

Figure S39. ^{13}C NMR spectrum of polyethylene obtained at polymerization temperature of 100 °C using **Ni^{OMe}** (entry 17, Table 3).

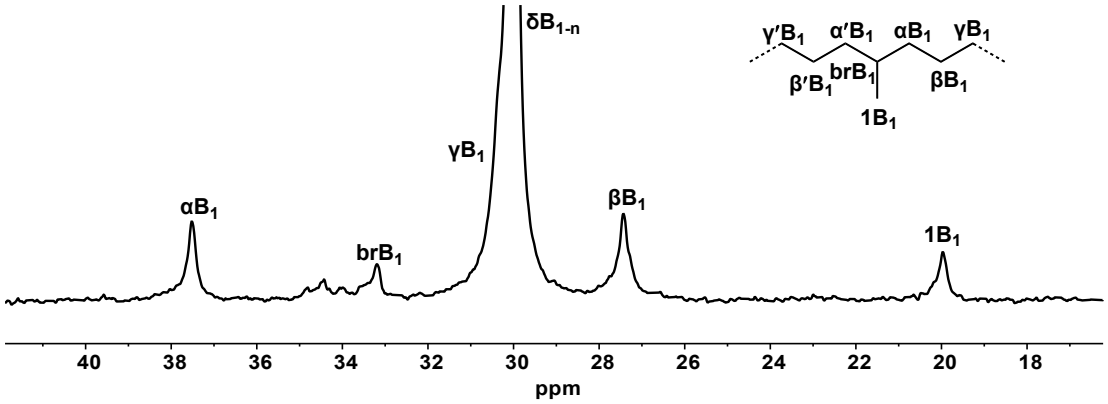

Figure 40. ^{13}C NMR spectrum of polyethylene obtained at polymerization temperature of 30 °C using **Ni^{PhF}** (entry 8, Table 3).

8. GPC curves of obtained polyethylene using different nickel complexes at different temperatures

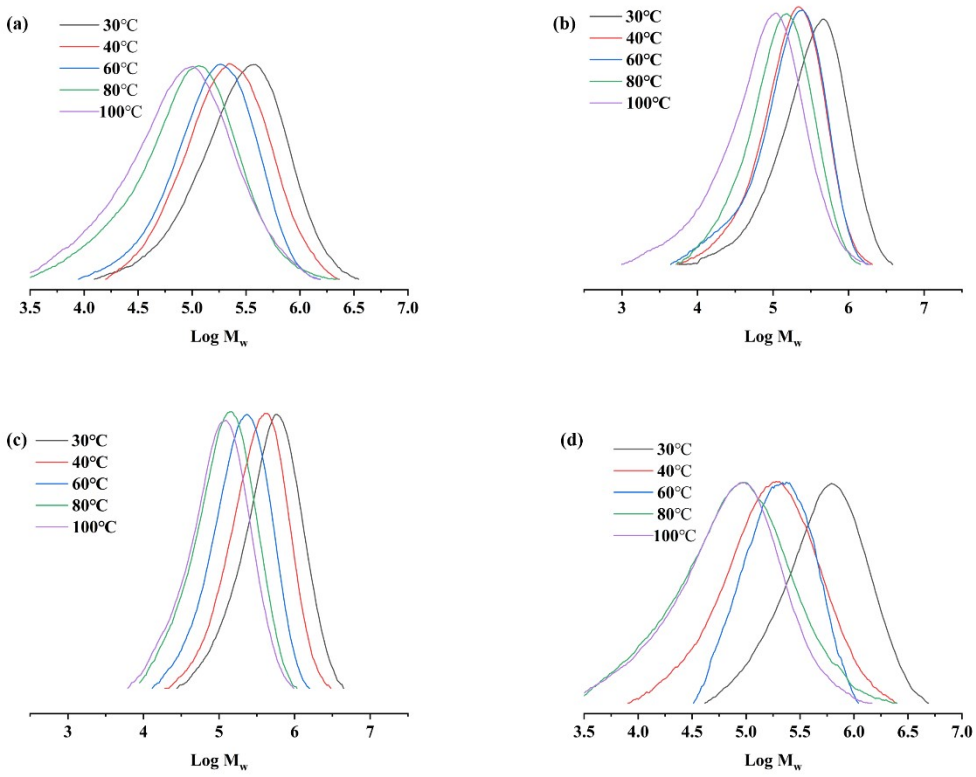

Figure S41. GPC curves of obtained polyethylene using **Ni^{Ph}** (a), **Ni^{PhF}** (b), **Ni^{PhOMe}** (c) and **Ni^{PhtBu}** (d) at different temperatures (entry 3-22, Table 3).

9. DSC curves of polyethylene at different conditions

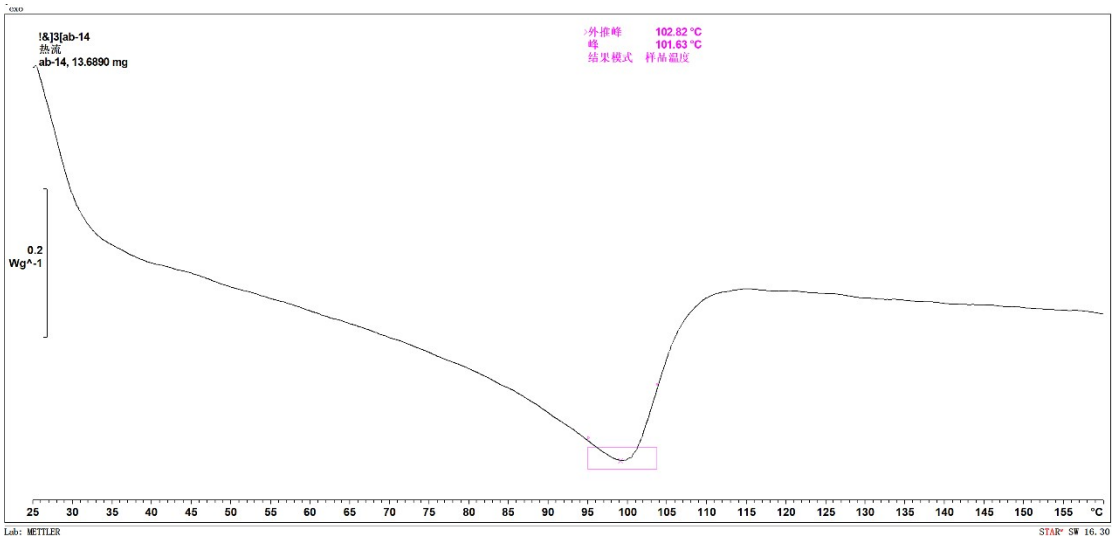

Figure S42. DSC curve of obtained polyethylene using **Ni^{PhF}**/MAO showing T_m. (entry 1, Table 1).

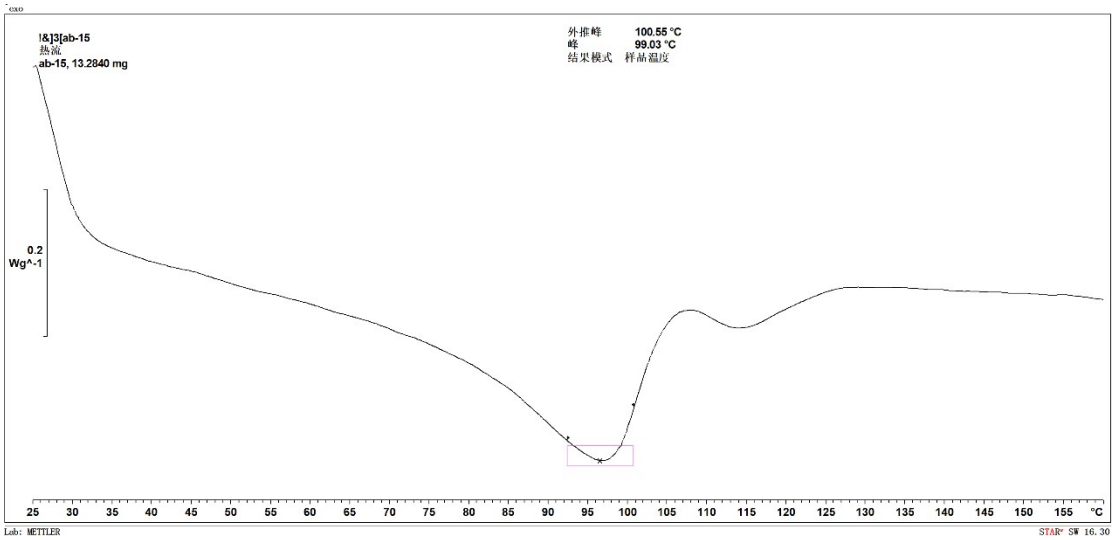

Figure S43. DSC curve of obtained polyethylene using **Ni^{PhF}**/MMAO showing T_m. (entry 2, Table 1).

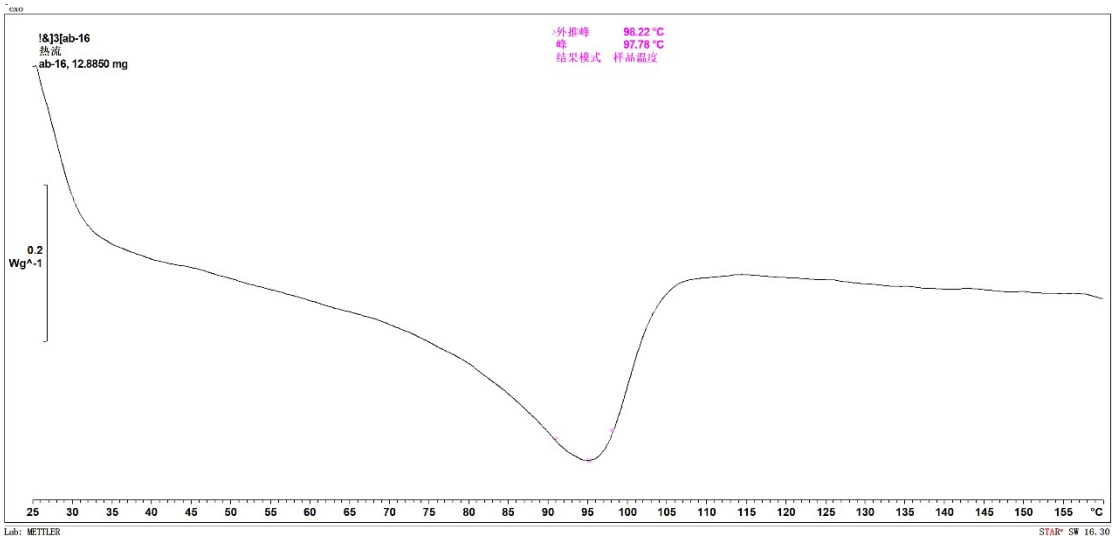

Figure S44. DSC curve of obtained polyethylene using **Ni^{PhF}**/DMAC showing T_m. (entry 3, Table 1).

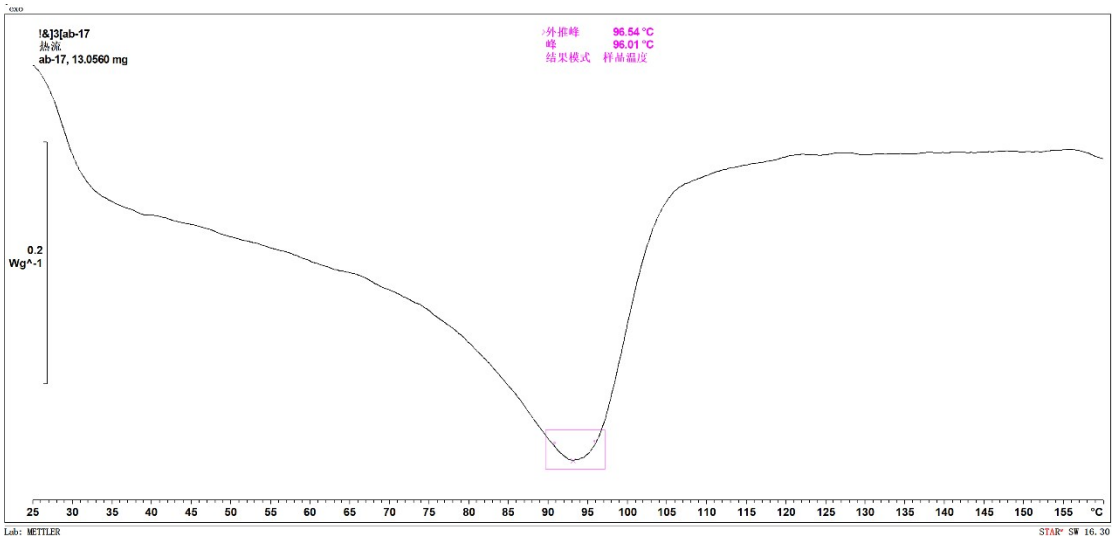

Figure S45. DSC curve of obtained polyethylene using **Ni^{PhF}**/DEAC showing T_m. (entry 4, Table 1).

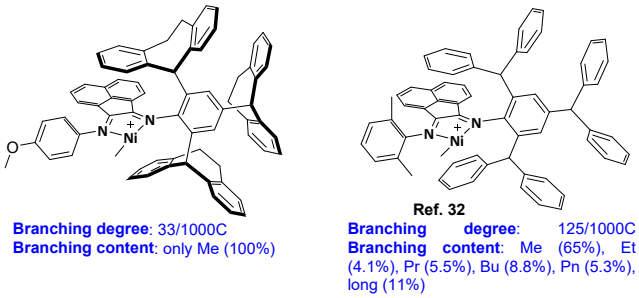

Figure 46. Comparison of branching degree with previously reported unsymmetrical α-diimine nickel precatalyst.

10. References

[1] Q. Muhammad, C. Tan and C. Chen, Concerted steric and electronic effects on α-diimine nickel- and palladium-catalyzed ethylene polymerization and copolymerization, Sci. Bull. 65 (2020) 300-307.
[2] G, M.; Sheldrick, SHELXTL-97, Program for the Refinement of Crystal Structures, University of Göttingen, Göttingen, Germany (1997).